Mechanical Characterization of Hydrogels and Biological Tissues in Unconfined Compression

by

Audrey Earnshaw

B.S., University of Colorado at Boulder, 2009

A thesis submitted to the

Faculty of the Graduate School of the

University of Colorado in partial fulfillment

of the requirements for the degree of

Master of Science

Department of Mechanical Engineering

2009

This thesis entitled:

Mechanical Characterization of

Hydrogels and Biological Tissues in Unconfined Compression

written by Audrey Lynn Earnshaw

has been approved for the Department of Mechanical Engineering

_____

Virginia Ferguson

_____

Stephanie Bryant

Date_____

The final copy of this thesis has been examined by the signatories, and we find that both the content and the form meet acceptable presentation standards of scholarly work in the above mentioned discipline.

HRC protocol # 1007.16

Earnshaw, Audrey Lynn (M.S., Biomedical Mechanical Engineering)

Characterization and Mechanical Properties of

Hydrogels and Biological Tissues in Unconfined Compression

Thesis directed by Assistant Professor Virginia Ferguson

Agarose and poly(ethylene-glycol) (PEG) are commonly used as scaffolds for tissue engineering applications (Mauck, 2002; Villanueva et al., 2008). This thesis work explores the differences in mechanical behavior between agarose, a physically cross-linked hydrogel, and PEG, a chemically cross-linked hydrogel, to set the foundation for choosing hydrogel properties and chemistries for a desired tissue engineering application. Agarose and PEG hydrogels form a porous solid, where the gel and the fluid together are expected to behave as a biphasic material with viscoelastic properties that are similar to many tissues (*e.g.,* articular cartilage and Wharton's jelly) (Saris et al., 2000). This thesis work also provides a tool that can be used to better understand PEG hydrogels and tailor the mechanical properties of PEG hydrogels to match those of the native tissue of interest. Native tissues experience both static and dynamic loading in a normal physiological environment. This thesis work focuses on characterizing properties of agarose and PEG hydrogels under both static (5-20% strain) and dynamic (0.01-10Hz) uniaxial unconfined compression.. The impact of variations in agarose and PEG composition on mechanical properties were investigated. Equilibrium modulus data for agarose 1-15% (w/w) and PEG (10-20% w/w) hydrogels showed variations between 5-575kPa and 46-313kPa, respectively. Complex modulus results for agarose and PEG hydrogels were found to be between 100-2,000Pa and 20-500Pa, respectively. A significant and direct correlation was found between weight percent (*i.e.,* composition) of the hydrogel precursors and corresponding stiffness. Higher polymer

fractions of hydrogels indicate higher water retention and perhaps fluid pressurization within the hydrogel. Although agarose and PEG hydrogels are both separately studied in the literature, this investigation provides one of the first comparisons of mechanical properties between the two materials. Despite the differences in the hydrogel structures (*i.e.,* physical versus covalent crosslinking), no statistical significance was found in the equilibrium modulus static tests between the two material types, inferring that both hydrogels performed similarly in terms of polymer composition driving mechanical behavior. Implications of this research may lead to new material research (*e.g.,* creating a composite of agarose/PEG) or alternative tissue engineering applications (*e.g.,* degradable drug delivery matrices that can withstand loading).

A secondary goal of this work was to investigate the compressive mechanical properties of Wharton's jelly found in the human umbilical cord. The lowest weight percent agarose hydrogel appears to most closely match Wharton's jelly in terms of viscoelastic behavior. Wharton's jelly plays an important role protecting the life-line of the umbilical cord between mother and fetus. Future work may pursue the feasibility of synergistically using an injectable hydrogel and growth factors to increase the compressive stiffness of the umbilical cord in high risk pregnancies (*e.g.,* pre-eclampsia or lean cords). The mechanical properties of Wharton's jelly a biphasic material that is similar to hydrogels, has not been thoroughly studied in the literature. Hydrogel testing was used in this study to provide the framework for validation of methods in characterizing Wharton's jelly.

Acknowledgement

Thank you to NIH (K22DE016608) and the D.O.E. GAANN fellowship for supporting part of this research.

Special thanks is extended to Virginia Ferguson and Stephanie Bryant for advising, Dr. Michael Plotnick and Dr. Virginia Winn for access to umbilical cord tissues, and Mark Czajkowski, Blair Dodson, Ryan Kennedy, Phil Kao, Chris Kloxin, Stephanie LaNasa, John Twomey, Megan Schroeder, Garret Nicodermus, and Chris Yakacki for providing help, assistance and instrumentation.

I would like to recognize Justine Roberts for her extensive willingness to help set up data collection and gathering, interpret results and continue to pursue the future work of this thesis.

Finally gratitude is extended towards my family, close friends and Dan Lebewitz for being supportive.

Contents

Chapters

Tables

Figures

1 Background & Significance

1.1 Hydrogels

Due to their high water content, hydrogels such as agarose and cross linked poly(ethylene glycol) PEG are commonly used as scaffolds for cell and tissue engineering applications (Bryant & Anseth, 2005). Gels synthesized from photo-reactive poly(ethylene-glycol) (PEG) macromonomers are well suited as cell carriers because they can be rapidly photo-polymerized *in vivo* by radical chain polymerization reaction under cell-friendly conditions. The high water content facilitates oxygen, nutrient, and waste diffusion, which makes gels ideal for culturing cells. Agarose is a natural biomaterial that is derived from agar and thought to be a slightly negatively charged polysaccharide (Rowley et al., 1999), which permits growing tissues in a three-dimensional suspension (Chen et al., 2004). Agarose can be physically cross-linked by heating and cooling (*e.g.,* similar to that seen with gelatin). Conversely, PEG hydrogel is a synthetic polymer that can be chemically modified with cross linkable groups and photo-polymerized under mild conditions without being toxic to cells. Hydrogels represent an ideal environment for testing purposes compared with biological tissues, enabling verification of testing protocols under controlled conditions without wasting valuable tissue that can be tedious and difficult to obtain.

Hydrogels are hydrophilic, cross-linked, and insoluble, except have the ability to swell in aqueous solutions (Bryant & Anseth, 2005). PEG hydrogels are highly cross-linked synthetic networks with controllable macroscopic properties. Photo-polymerization of multi-functional monomers or macromers in the presence of photo-initiator forms a three dimensional network via radical chain polymerization to produce a cross-linked gel.

Uniaxial compression testing is a common method used to determine mechanical behavior of tissue. Because confined compression only shows change in one dimension, limited information can be determined about the mechanical properties of the test material. Therefore, unconfined compression was used to study the deformation of the hydrogel as it deformed freely in three dimensions. It is important to do both static and dynamic tests on hydrogels to mimic physiologically similar mechanical characteristics. Physiological loading levels have been well characterized in some tissues (*i.e.,*articular cartilage). Contact stresses in healthy joints typically range from 1 to 6MPa for light to moderate daily activities (Herberhold et al., 1999; Kaab et al., 1998). Under more strenuous activities, peak contact stresses in joints have been estimated to reach 12MPa (Matthews et al., 1977).

Understanding the mechanical properties is essential for developing biomedical applications. Important properties include the equilibrium modulus, dynamic stiffness, failure stress and strain in tension and compression as a function of molecular weight, stress relaxation, fluid pressurization, and hydraulic permeability (Gu et al., 2003. Often the mechanical properties of hydrogels and similar soft tissues are deformation dependent. Agarose hydrogels presumably follow linear biphasic mixture theory (Gu et al., 2003).

1.1.1 Agarose

Derived naturally from seaweed, agarose is and can be used as a gelling agent or soup thickener. Furthermore, agarose is a polysaccharide based polymer that is slightly negatively charged with sulfate groups and has a double helical network that is stabilized by water molecules. Below is an example of a linear galactan hydrocolloid (agarose), which is a linear polymer containing alternating D-galactose and 3,6-anhydro-L-galactose units (A9539, Sigma-Aldrich, Saint Louis, Missouri, 2009).

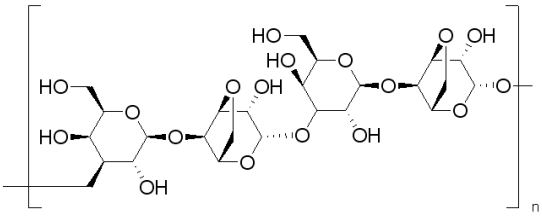

Figure 1.1 Chemical Structure of agarose

Agarose is a well documented material in the literature as an elastic material that can be used to validate mechanical methods (Chen, 2005; Gu, 2003; etc.). It is noted that equilibrium modulus values for agarose gels with the same concentrations can vary significantly depending on the source of agarose and batch-to-batch variations (Gu et al., 2003). Common molecular weights are approximately 120,000. Biology-grade agarose, which includes random molecular sizes and lengths, was used for this thesis research to minimize the variations seen batch-to-batch in the literature.

1.1.2 PEG Hydrogel

PEG is thought of as elastic, and traditionally used in skin creams, as a lubricant, or laxative in its uncrosslinked form. Macromer chemistry influences the hydrophilicity solvent-polymer interaction or overall water content in PEG hydrogel (Bryant & Anseth, 2005). A synthetic monomer PEG (molecular weight of 4,600) was used in this thesis for cytotoxicity reasons. For clarification purposes, once PEG (*i.e.,* a non toxic polymer) is modified with methacrylate groups to produce PEG dimethacrylate size becomes an issue with toxicity. The molecular weight plays a role in gel structure and degradation. A disadvantage of higher molecular weights is a decrease in the cross-linking density. The highest degree of functionality for PEG hydrogel is due to having two hydroxyl groups. PEG has two hydroxyl groups at each end (the minimum required to form a cross-linked network) of the polymer, where each end can be modified with a vinyl

group to produce a divinyl macromer. The PEG molecule acts as a cross-link between the kinetic chains. The PEG hydrogels are photo-chemically cross-linked with ultra-violet (UV) light. The type of initiator responding to UV light and other conditions used are important because the initiator controls the polymerization rate and influences the final gel structure. A disadvantage of using radical initiation is that oxygen inhibits the radicals from forming bonds (Bryant & Anseth, 2005).

1.2 Biphasic Theory

Biphasic theory consists of a soft porous compressible phase and an incompressible fluid phase. Hydrogels, such as agarose and PEG, are characterized by the number of bonds, or cross-links, in the polymer chains present within the gel (solid phase) and the amount of fluid present such as phosphate buffered saline (PBS) (fluid phase). The amount of fluid retained depends on the chemical potential within the sample of interest. Water is attracted inward and balanced by a retractile cross-linking force that restricts water (Bryant & Anseth, 2005). Wharton's jelly's biphasic phases would include collagen and ground substance (soft porous phase) and interstitial fluid (liquid phase). Considering composition, molecular structure, water content and electrolytes, the frictional drag of interstitial flow through a porous-permaeable collagen-proteoglycan solid matrix was found to be the most important factor governing the fluid/solid viscoelastic properties of articular cartilage in compression (Mow et al., 1980; Mow et al., 2004).

During mechanical compression testing, observed volume changes occur from fluid leaving the tissue. The importance of experimentation between solid and porous platens must be investigated to determine whether there is a statistical difference in mechanical properties between the two setups. Porous platens allow fluid to flow into the platen while

the poroelastic sample is under mechanical deformation. Allowing fluid to exude into the platens will provide the most compaction of the solid phase, which may provide more accurate characterization of mechanical properties (Mow et al., 2004). Conversely, solid platens allow no such fluid penetration, resulting in less compaction of the solid phase, and potentially different empirical results. Biphasic viscoelastic properties cannot be predicted due to strains in three dimensions and therefore must be found empirically by fitting experimental data and calculating the stress (Knapp, 1997).

1.3 Human Umbilical Cord & Wharton's Jelly

Importance of the subject:

The human umbilical cord is composed of one vein and two arteries wrapped in a sheath of Wharton's jelly. The umbilical cord is subject to many forces during normal fetal movements and uterine contractions such as twisting, pulling, and compression. Wharton's jelly is frequently described as a mesenchymal or mucous connective tissue. There is no shortage of literature describing Wharton's jelly qualitatively in terms of composition and ultrastructure. What the literature lacks is quantitative and qualitative findings relating the compressive biomechanical behavior of Wharton's jelly. More research on Wharton's jelly is clinically pertinent in terms of better diagnostic measures to assist in prevention of cord accidents in high-risk pregnancies due to abnormalities that may be caused either genetically or pathologically. Literature suggests that proteoglycans, glycosaminoglycans, hyaluronic acid, and collagen play key roles in the biomechanical behavior of the Wharton's jelly in compression of the human umbilical cord (Gervaso et al., 2003). The effects these components have on the mechanical response of the extracellular matrix are essential to

understanding the macro-level scale of the Wharton's jelly's role in protecting the umbilical cord.

Wharton's jelly at the molecular level is beginning to be studied more in-depth in terms of proteoglycans, glycosaminoglycans, hyaluronic acid and collagen. Proteoglycans do not have a preferred orientation and contain an abundance of binding sites between covalently bound proteins and glycosaminoglycans (GAGs) (Humphery & Delange, 2004). Proteoglycans also bind to growth factors such as described in Table 1.1.

Table 1.1: Description of growth factors and their associated functions.

Growth Factor	Function
Fibroblast Growth Factor (FGT)	Wound healing and embryonic development
Transforming Growth Factor (TGF)	Wound healing and embryonic development
Insulin Growth Factor (IGF)	Cell growth (inhibits cell apoptosis)
Epidermal Growth Factor (EGF)	Growth and differentiation
Platelet-Derived Growth Factor (PDGF)	Regulates cell growth and division, blood vessel formation (activation or inhibition)

GAGs are linear polymers with repeating disaccharide units. GAGs occupy a large volume because they are highly negatively charged, which causes considerable water retention in the extracellular matrix thus, allowing cells to withstand significant compressive loads (Humphrey & Delange, 2004). Hyaluronic acid is a non-sulfated glycosaminoglycan that plays a significant role in cell growth and migration. Hyaluronic acid is highly negatively charged as well, which aids in enormous water retention within Wharton's jelly. Wharton's jelly is ninety percent water and is responsible for cell resilience (ability to absorb energy and recover) against compression and vibration (Skulstad, 2005). There are five major

collagen types: I, III, and IV are found in Wharton's jelly, with types VII and XIX also being found intermittently (Myers et al., 2003) where each type of collagen differs in its mechanical and physiological role in the body described in Table 1.2.

Table 1.2: Collagen types and locations.

Collagen Type	Location
Type I	Many organs and system's extracellular matrix (such as in tendon, skin, bone, and the blood vessel walls according to (Marcu et al., 2000) serving as a protective structure against sudden movement (Buttafoco et al., 2006).
Type III	Variety of muscular and elastic tissue, such as artery, uterine leimyoma, and skin (Marcu et al., 2000). In the human umbilical cord, type III is found in the amniotic epithelium, Wharton's jelly, smooth muscle cells of the vein and arteries, and the endothelial basement membrane areas (Myers et al., 2003).
Type VII	A minor type of collagen found in anchoring fibrils, expressed by keratinocytes found in human umbilical cord. This type of collagen was found analyzing the fibroblast-like cells from Wharton's jelly (Marcu et al., 2000).
Type XIX	This is nonfibrillar, scarce, and found in the amniotic epithelium, Wharton's jelly, smooth muscle cells of vasculature, and endothelial basement membrane areas (Myers et al., 2003). This is a new discovery showing morphology resembling long, rod-like structures with many kinks (Myers et al., 2003).
Type XIX	Spongy network of interlacing collagen fibers that appear as a wavy network with random small woven bundles (Vizza et al., 1996). There is a wide system of interconnected cavities that include "canalicular-like" structures as well as a "cavernous" and "perivascular space" (Vizza et al., 1996).

The amount of collagen in Wharton's jelly plays a direct role in the viscoelastic behavior. The amount of cross-linking is a key indicator of stiffness (Gervaso, 2003).

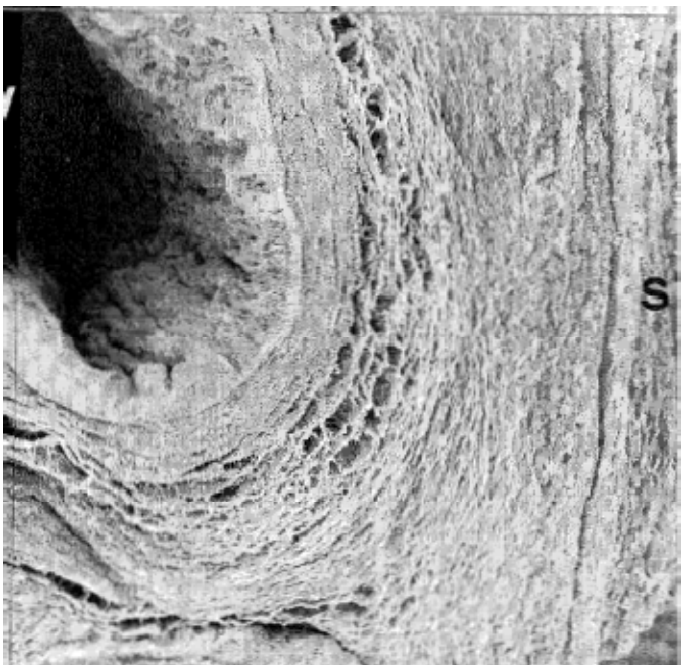

Figure 1.2: Scanning Electron Microscopic image of decellularized Wharton's jelly showing the collagen backbone. The 'S' refers to the amniotic epithelium layer. Different layers are shown starting at the outer wall "S" and moving toward the center of the vein at X35 Magnification (Vizza et al., 1996).

Wharton's jelly is shown using a three dimensional high-resolution scanning electron microscope (SEM) in Figure 1.2. The photo suggests (moving inward from the outside) compartmentalization broken down into the amniotic epithelium layer, "cavernous space", "canicula-like" structures, and a perivascular regime. Just beyond this layer into the Wharton's jelly there is a spongy network composed of both cavernous spaces and canicula-like structures. The cavernous spaces have a dense interstitium, a continuous network of single fibrils. Within this interstitium the collagen appears to be organized in condensed wavy bundles. It is noted that this area may contain basement membrane and other cellular elements that may influence the movement and size of umbilical vessels. The innermost part of the Wharton's jelly within the cord shows additional wavy collagen bundles and interlaced fibrils. The canicula-like structures are oriented cordially with respect to the vessel. Fibril branches connect these structures, which may be involved in the redistribution

of ground substance and nutrients. The next area inward is the "perivascular space" acting as a boundary between the collagen skeleton and vein. There are thick collagen bundles that cross the perivascular space connecting the vessels. Perivascular space allows the vessel flexibility to move and change morphology, which may also act to dampen forces in a protective way (Vizza et al., 1996).

The internal compartments allow Wharton's jelly to adapt to external compressive loads on the cord. During compression or twisting, the ground substance flows through the canalicula-like structures into the spongy spaces, or large cavernous spaces, redistributing the volume and preserving blood flow through the vessels. The structure can be described as a semi-rigid erectile tissue (Vizza et al., 1996).

There are several types of compression that may occur in the human umbilical cord such as nuchal loops, umbilical cord prolapse, knots, and cord entanglement in the case of twins. According to the March of Dimes, nuchal loops (25% of all babies born), umbilical cord prolapse (1 out of every 300 births) and knots (about 1% or more of all babies born) result in 5-10% of stillbirth cases. Compression is a serious occurrence, which can cut off vital oxygen supply to the fetus, resulting in permanent brain injury or death.

If the umbilical cord is completely compressed one time for a period of one minute, it will take five times as long for the cord to recover (Gervaso, et al., 2003). During fetal movement deforming the cord (compression, twisting or stretching) venous flow is notably decreased over a constant hydraulic pressure drop (Gervaso et al., 2003). Compression of the cord can interfere with nutrient delivery and waste disposal as well as increase the fetus's heart rate.

It is still unclear how a compressive force is distributed within the cord. Literature suggests that the water is displaced to other areas of the Wharton's jelly. Proteoglycans, glycosamionglycans, hyaluronic acid and collagen play a key role in the biomechanical functions of the extracellular matrix. Mechanical stimuli have a direct influence on gene expression in different cell types including chondrocytes, endothelial cells, epithelial cells, fibroblasts, macrophages, myocytes, and osteoblasts (Humphery & Delange, 2004). It is unknown to what extent the proteoglycans, hyaluronic acid or glycosaminoglycans play in water retention of Wharton's jelly as well as effective cross-linking of the different types of collagen on the extracellular matrix.

1.4 Motivation/Aims

- Demonstrate how the composition and weight percents of a hydrogel drive compressive mechanical behavior.
- Show that hydrogels and Wharton's jelly from the umbilical cord demonstrate similar patterns of mechanical behavior and that hydrogels may serve as a suitable reference for interpreting more complex biological tissues.
- Explore the differences in chemical and physical cross-linking between agarose and PEG in terms of mechanical behavior.

2 Materials and Methods

2.1 Agarose Gel Preparations

Hydrogels were formulated from the following weight percents: Agarose 1, 5, 10, 15% (w/w) and PEG 10, 15, 20% (w/w) with an n=3/group. Hydrogel synthesis took place in cylindrical tubes that were cut to 5mm heights and allowed to free swell in PBS for ~24 hours. Uniaxial mechanical testing was performed on submersed gels in unconfined compression, including both static and dynamic tests as described in this thesis.

2.1.1 Preliminaries

Agarose gels were generated using a combination of agarose powder (A9539, Sigma-Aldrich, Saint Louis, Missouri), 1X PBS (phosphate buffered saline, without magnesium or calcium) and heat to make the following weight percents found in Table 2.1.

Table 2.1: Formulated agarose concentrations that were mechanically tested and compared to the current literature.

Concentration (%w/w)	Weight (g)	Volume (ml)	%
1.0	0.20	20	100
5.0	1.00	20	100
10.0	2.00	20	100
15.0	3.00	20	100

2.1.2 Agarose Synthesis

Agarose was continuously stirred in a double boiling water bath, to prevent charring, until the solution turned clear. To reduce bubbles, weight percents greater than 1% (w/w) were placed in a heated vacuum (~90 ºC). The 15% agarose hydrogels

required additional PBS prior to a series of vacuum cycles. Pre and post vacuum weights of agarose were noted to ensure the desired weight percent. Beakers were capped and placed in a heated vacuum cycle between 50-55ºC to prevent gelling. Vacuum compression and decompression did not exceed 5mmHg /min, which reduced bubbling and gel growth. Agarose gels were formed by allowing the gel to cool inside 5mm diameter syringes.

2.1.3 Agarose Molds

Syringes were used to suction liquid agarose into the 5mm cylindrical mold. The 15% (w/w) agarose is very viscous and required manipulation and twisting to minimize air suctioning up into the syringe. Agarose syringes were capped with paraffin, to prevent dehydration, and allowed to cool to room temperature upright. The agarose syringes were then placed into a 4ºC refrigerator for a minimum of 10 minutes.

Cylindrical Teflon molds and a razor blade were used to align and cut the agarose gels perpendicular to their axis to achieve 5mm heights. Agarose samples were immediately placed in PBS to maintain gel hydration and allow free swelling for a minimum of 24 hours prior to testing.

2.2 Poly(ethylene glycol)PEG Preparation

2.2.1 PEG Methacrylation

A recent accepted method for synthesizing poly(ethylyne glycol) dimethacrylate using a microwave methacrylation method was used (Lin-Gibson et al., 2004; Nicodemus et al., 2008). PEG monomer (2.5g, MW 4600g/mol, Sigma-Aldrich, Saint Louis, Missouri) was microwaved with methacrylic anhydride (400W for 5 minutes) in a microwave-resistant glass vial with trace amounts of hydroquinone (Sigma-Aldrich, Saint

Louis, Missouri) until molten and purged with argon gas for 1 minute. Hydroquinone, an inhibitor, kept the solution from polymerizing by quenching free radicals that may initiate polymerization. The amount of methacrylic anhydride (10:1mol MA:mol PEG, Sigma Aldrich, Saint Louis, Missouri) was calculated using the sample calculation below:

Amount of Methacrylic Anhydride (MA) =

$$\frac{(2.5\text{ g PEG})(\text{mol PEG}/4600\text{g})(10\text{mol MA /mol PEG})(154.17\text{g/mol MA})(1/0.94)}{(1.042\text{g/ml})} \quad (1)$$

$$= 0.855\text{ml MA per vial} \quad (2)$$

$$MW_{MA} = 154.17\text{g/mol at 94\% purity (714}\mu\text{L/vial)} \quad (3)$$

$$\rho_{MA} = 1.042\text{g/ml} \quad (4)$$

After microwaving (~10min), the solution was allowed to cool at room temperature while the reaction completed. The contents were then microwaved again (~5min, 400 W) to liquefy the contents. Before the solution solidified, chilled methylene chloride (20ml, CH_2CL_2, Sigma-Aldrich, Saint Louis, Missouri) was added to dissolve the PEG dimethacrylate (PEGDM).

The product was precipitated from solution three times in ice-cold ethyl ether (100ml of ethyl ether per 10ml of PEGDM in methylene chloride) by pouring the precipitated product through a filter (Whatman #4) and ceramic funnel into a beaker below. The product which was very light sensitive was wrapped with aluminum foil with air gaps to allow breathability. The air-dried powder was further dehydrated with a vacuum oven overnight at room temperature to remove the residual ethyl ether.

2.2.2 Purifying Dialysis

Dialysis was performed according to the manufacturer's protocol (Spectra por, Rancho Dominguez, CA) on 4600MW + 100MW = 4700MW of product. Dialysis works

by purifying the product by removing acids and salts over a concentration gradient resulting in 15% less product. If the product weighed less than 500mg it was discarded. The DI water was changed at least 4 times, every 1-2 hours.

Dialysis tubing (500 MWCO) was soaked for 30 minutes prior to adding the product to enable preservatives in the tubing to leach out and then were rinsed. Polymer was weighed (*i.e.,* 4.285g) and dissolved in DI water (5-10% w/v) (*i.e.,* 42ml of DI water). Liquid polymer (13ml) was added to each vial of plastic tubing and clamped with a magnetic clip at one end. A non-magnetic clip was placed on the other end of the tub and clipped to the edge of the beaker so that the DI water could continuously be stirred.

2.2.3 Freeze Dry

Following dialysis, the liquid polymer was placed in a freeze flask to flash freeze (sublimation) the contents and remove the water converting the PEGDM into a fine powder that is 30% more stable. The lid was properly secured on the flask (< 10ml) and placed on the lyophilizer (-40ºC) in a high vacuum for 48 hours.

2.2.4 Photopolymerization

PEGDM was dissolved in PBS (1X Gibco Dulbecco's PBS sterile, Carlsbad, CA) at the desired weight percents in Table 2.2 and mixed with Photoinitiator (PI) (Irgacure I2959, Ciba-Geigy, USA). A small amount of PI (stock was 0.6 wt% in PBS) was used to minimize the effect of cytotoxicity in cellular applications due to increased temperature upon radical UV photo-polymerization. PEG hydrogels were made at the weight percents outlined in Table 2.2.

Table 2.2: Weight percent of polymer and desired gel concentration.

Concentration (w/w)	Weight Percent of Photoinitiator (PI)
10% gel	0.05 wt%
15% gel	0.0222 wt%
20% gel	0.0125 wt%

Further calculation is in Appendix A, demonstrating the amount of PBS, PI, and PEGDM to add for each desired gel concentration in Table 2.2. After vigorously stirring the ingredients, the solution was placed in 5-mm diameter syringes (used as molds) and capped with paraffin. Photopolymerization occurred under UV light (365nm, 6mW/cm^2) for 10 minutes. The reaction was exothermic and chemically cross linked the molecule. Samples were cut into 5mm diameters as described previously.

2.3 Matlab – Mechanical Testing

Custom Matlab programs were written to analyze both the static and dynamic tests. The code can be found in Appendices D and E. Each program reads the data stored on the test machine and separates the data into arrays for further calculations. Mechanical tests were performed with a customized Bose Mechanical tester adapted from an Electro-Force 3200 (Bose, Praire, Minnesota).

2.3.1 Equilibrium Modulus Analysis

Three specimens each of 1%, 5%, 10% , and 15% (w/w) agarose and 10%, 15% and 20% (w/w) PEGDM were submerged in 1% Mg^+ or Ca^{2+} free PBS (*i.e.,* phosphate buffered saline) at room temperature. Unconfined compression testing was performed using solid metal platens at an initial loading rate of 5mm/s. A series of stress relaxation

equilibrium modulus tests were performed at 5% strain increments from the initial height (30 minutes each) to a total depth of 20% the initial height (Figure 2.1 (A)).

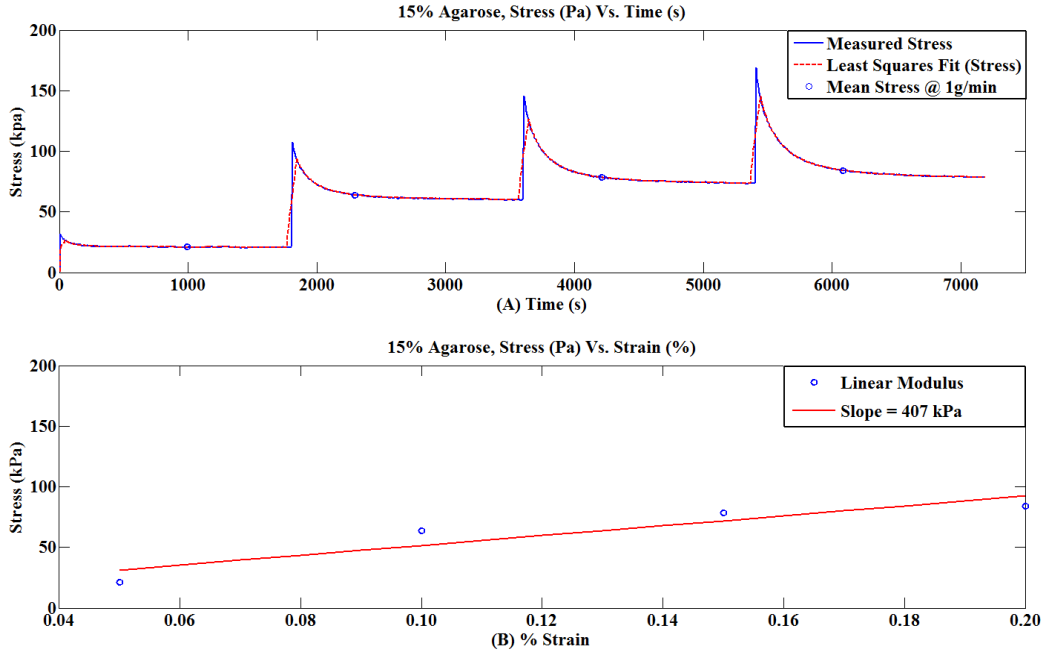

Figure 2.1: (A) Representative incremental stress relaxation curve for 15% (w/w) agarose. (B) Representative plot of equilibrium modulus for 15% agarose gel yielded a slope of 407kPa.

The test data is shown with a solid line (termed 'Measured Stress' in Figure 2.1 (A)). A custom Matlab program was written to smooth the data with a least squares fit. The mean stress at each strain increment was recorded when a change of ≤ 1g/min was reached. The recorded points at equilibrium in Figure 2.1 (A) were plotted and fit to a line equation to produce the equilibrium modulus (Figure 2.1 (B)).

2.3.2 Dynamic Modulus Analysis

Three specimens each of 1%, 5%, 10%, and 15% (w/w) agarose and 10%, 15% and 20% (w/w) PEG were submerged in PBS at room temperature. Dynamic unconfined compression testing was performed using solid metal platens at frequencies ranging from 0.01 – 10Hz. The frequency range can be thought of in terms of the impact that a

material may encounter during normal human movements from walking to running. Seven logarithmically varying frequencies were chosen (0.01, 0.05, 0.10, 0.50, 1.00, 5.00, 10.00Hz) and applied from a high to low frequency to collect 400 data points each. A series of frequency sweeps were performed at 10% strain of the initial height.

Phase lag exists when materials being tested are not perfectly elastic and exhibit dissipative energy loss after each sinusoidal cycle (Lakes, 1999). Assuming linear viscoelastic behavior at equilibrium the stress and strain both vary sinusoidally with the strain lagging behind the stress (Ward and Sweeney, 2004).

$$\epsilon = \epsilon_0 \sin(\omega t) \tag{5}$$

$$\sigma = \sigma_0 \sin(\omega t + \delta) \tag{6}$$

Where ω is the angular frequency and δ is the phase lag. The custom Matlab program allowed viewing the raw data of the seven plots in addition to allowing only collection of areas of choice that were visually in equilibrium. The equilibrium data was taken at the specified ranges and a phase lag was calculated for each frequency. For visualization purposes, plots of the phase lag at each frequency were generated by plotting stress versus strain. The area within the stress-strain curve represents dissipative energy or viscous effects (Lakes, 1999). Viscous effects have been encountered when cartilage dampens the force on joints from an exerted load (Park, 2004). The amount of viscous effects can be viewed in the graphs found in Appendix E. G_1 and G_2 are the storage and loss modulus, respectively, derived from expanding out the stress equations describing linear viscoelastic behavior.

$$\sigma = \epsilon_0 G_1 \sin(\omega t) + \epsilon_0 G_2 \cos(\omega t) \tag{7}$$

$$G_1 = \frac{\sigma_0}{\varepsilon_0} \cos(\delta) \tag{8}$$

$$G_2 = \frac{\sigma_0}{\varepsilon_0} \sin(\delta) \tag{9}$$

G_2 is 90º out of phase with G_1. The diagrams in Appendix E provide a master curve that has incorporated how the energy is stored or dissipated over the seven frequencies. Tan delta, the ratio of G_1 and G_2, provided a ratio of elasticity to dampening, used to indicate the level of elasticity of the specimen.

$$\tan(\delta) = \frac{G_2}{G_1} \tag{10}$$

G* or the complex modulus was defined in terms of magnitude of G_1 and G_2.

$$G^* = (G_1^2 + G_2^2)^{1/2} \tag{11}$$

Stress relaxation occurs when a viscoelastic material is displaced at a controlled rate and then held constant. The viscoelastic material will respond by relaxing to relieve stress (Mow et al., 2004). This phenomenon is common in biological tissue and can be seen in the data supplied in Appendix E. Conversely, tissues exhibiting creep phenomena will show an increase in deformation under a constant applied stress (Mow et al., 2004).

2.4 Wharton's Jelly Preparation

Ethical approval was obtained from the University of Colorado Institutional board for the collection of Wharton's jelly from human umbilical cords. Tissue was obtained via informed consent from subjects delivering full term, healthy babies at the Boulder Community Hospital. Tissue from each umbilical cord was tested within 72 hours of delivery. The umbilical cords were stored in 1X PBS in a 4ºC refrigerator. Wharton's jelly specimens were collected using a 5-mm biopsy punch, taken longitudinally along the axis of the cord between the three vessels as shown in Figure 2.3. It is noted that punching a uniform 5-mm section of tissue was very difficult as the material frequently slipped, curled

and deformed while trying to cut samples. The cords also seemed to have internal coiling stresses that prevented the tissue from having a flat surface to make excisions from.

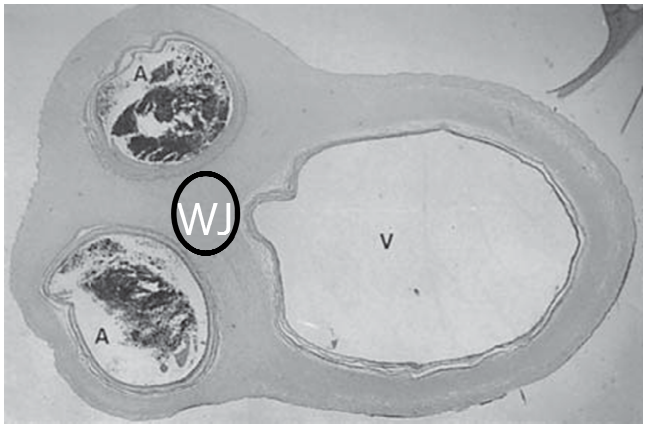

Figure 2.2: Human umbilical cord showing two arteries and one vein. The Wharton's jelly was punched in the center of these three vessels to ensure a homogeneous sample (Vizza et al., 1996).

3 Prior Work on Umbilical Cord Tissues

Dynamic mechanical analysis (DMA-7E, Perkin Elmer, Shelton, Connecticut) was used initially to try to characterize uniaxial loading of equine Wharton's jelly in unconfined compression. A 13-mm cup with a 10-mm plate (Perkin Elmer, model number N5390467) and a 21.5-mm cup with a 20-mm plate (Perkin Elmer, model number N5390468) were used for static force, creep and frequency scans to obtain properties such as stress, strain, storage modulus, loss modulus, complex modulus, and tan delta. Figure 3.1 demonstrates a 70% EtOH solution being used as an experimental control to dehydrate the tissue during testing. Repeatable results were unobtainable due to the limited sensitivity of the DMA both in set-up and execution of tests. Often times, samples would be destroyed from problems with the automated sensing of the sample height. Experiments were aimed at performing mechanical tests on samples of Wharton's jelly and verifying the analysis with images from a low vacuum scanning electron microscope. The samples of Wharton's jelly would allow differentiating the roles that proteoglycans, hyaluronic acid, and glycosaminoglycans played in interaction with water. Samples were immersed in varying concentrations of ethanol to quantify the effects of hydration on the extracellular matrix as well as varying concentrations of aldehyde to enhance cross-linking of the collagen compared to the natural state of the tissue.

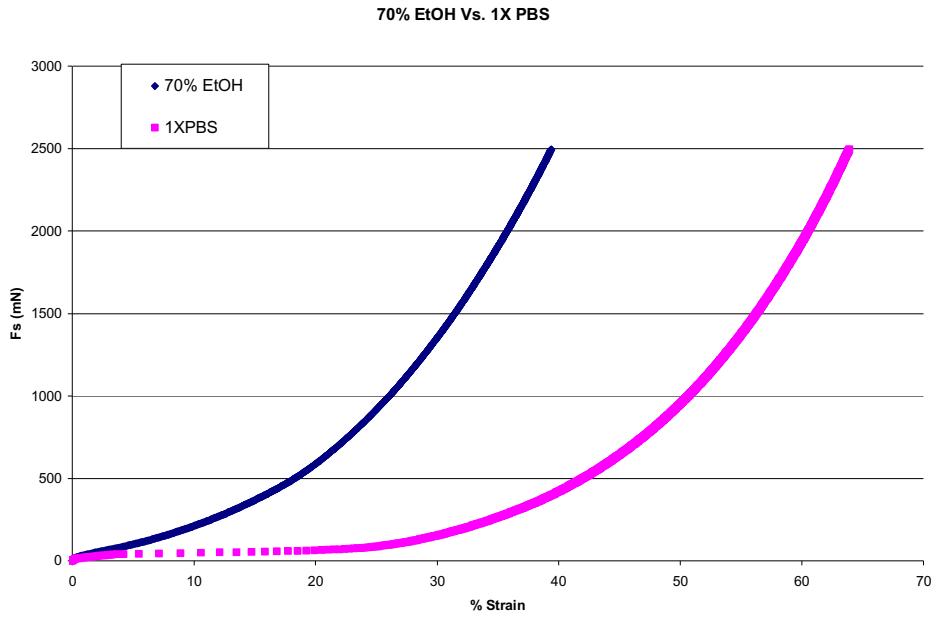

Figure 3.1: Demonstrates equine tissue submersed in 70% EtOH having a stiffer mechanical response to compressive loading.

A creep test was also performed to observe viscoelastic behavior as shown in Figure 3.2. A force of 1300mN was applied at a very quick rate to the tissue in uniaxial unconfined compression and held for 20 minutes as seen. The tissue rapidly responded in a non-linear fashion reaching 65% strain from its initial height. Afterwards the load was removed, allowing the tissue to relax for an additional 20 minutes. The tissue never fully recovered and non-linearly descended to approximately 600mN, at 33% strain.

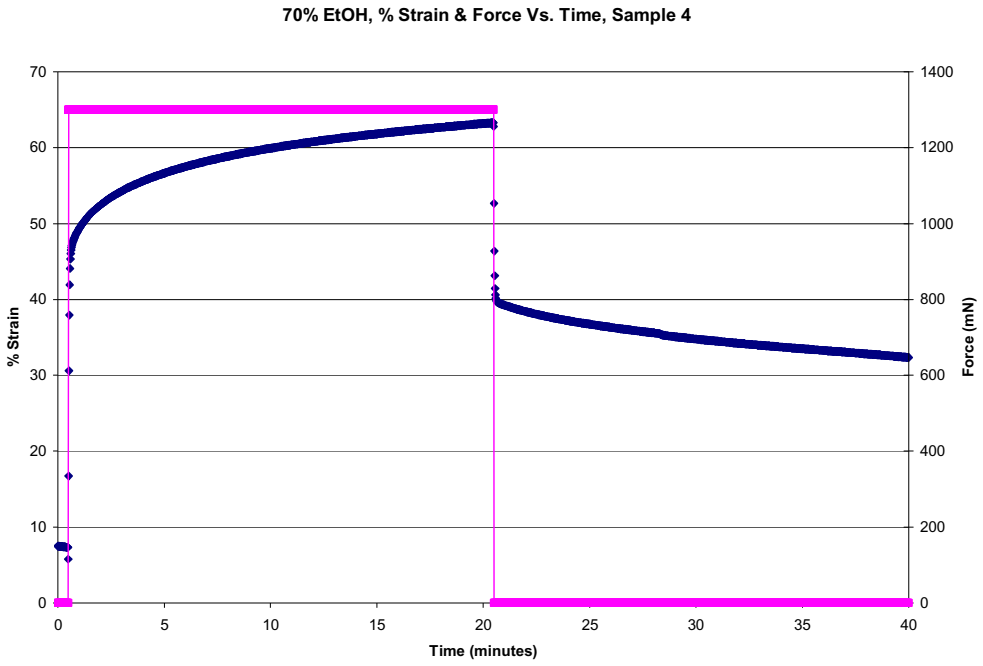

Figure 3.2: Illustrates a creep test applied over 20 minutes and allowed to recover for the same amount of time.

A number of assays were examined for feasibility of testing such as indentation, rheometry, and another type of DMA Q800 (TA Instruments, New Castle, Delaware), and MTS Insight II (MTS Systems Corporation, Eden Praire, Minnesota). Indentation instruments at the University of Colorado did not have the proper sensitivity, required for soft tissue, to be able to perform the tests of interest. A rheometer was also used; however Wharton's jelly was not stiff enough to obtain usable data. The Q800 testing system was investigated and found to have the sensitivity required, but an additional fixture was not within the budget of this study. An Insight II was used to statically compress agarose gels. A program was written to perform static submerged uniaxial unconfined compression with a "pulsatile-dynamic" load and no-load period to try to replicate published results for agarose gels (Scandiucci de Freitas, 2006). Difficulties with this approach consisted of accurately securing the sample in place prior to and during testing. Another disadvantage of using the Insight II

was the limitation of not being able to perform a dynamic test. Finally, a customized Bose Mechanical Testing System in the Chemical Engineering Department, in Professor Bryant's Lab, became available. The Electro-Force 3200 (Bose, Praire, Minnesota) had the required sensitivity and could perform both static and dynamic tests very accurately.

4 Results

4.1. Overview

Agarose and PEG hydrogels as well as Wharton's jelly samples were both statically and dynamically tested with a Bose Mechanical Tester. Equilibrium modulus results were obtained from static tests in which the sample was compressed at different heights (5, 10, 15, and 20% of the initial gel height) and held constant for 30 minutes. G_1, G_2, tan(δ), and G* were derived dynamically at seven different frequencies (10, 5, 1, 0.5, 0.1, 0.05, and 0.01Hz) at 10% between 10 ± 2.5% of the initial gel height.

4.2 Agarose and PEG Results

4.2.1 Equilibrium Modulus

Equilibrium modulus results were statistically different for both Agarose and PEG hydrogels. The material *type* significantly influenced measured values of equilibrium modulus. Agarose produced a substantially larger equilibrium modulus value at 10 and 15% (w/w) than PEG at 10 and 15% (w/w). Additionally, agarose and PEG hydrogel, equilibrium modulus's increased with weight percent as visualized in Table .

Table 4.1: Equilibrium modulus for agarose and PEG hydrogels (n=3/group). Data are presented as Mean ± SD.

Mean Equilibrium Modulus ± Standard Deviation (kPa)					
Concentration (w/w)	***1%***	***5%***	***10%***	***15%`***	***20%***
Agarose	5 ± 1	133 ± 32	345 ± 45	575 ± 139	-
PEG	-	-	46 ± 3	201 ± 25	313 ± 90

4.2.1.1 Statistics

A summary of the equilibrium modulus values are presented in Table 4.1. One-way ANOVA ($\alpha = 0.05$) was used to compare equilibrium modulus values within agarose or PEG. Significant differences existed only between each weight percent of both agarose ($P < 0.001$) and PEG ($P < 0.001$). There was no significant difference found between material types. The statistical software used was SigmaStat V2.03 (SPSS Inc., Chicago, Illinois).

4.2.2 Dynamic Modulus

A stress-relaxation phenomenon was observed during testing and can be visualized from the plots found in Appendix E. A compressive strain was applied and oscillated between 8.5 and 12.5% of the gel's initial height. The force response increased with time (compression is negative), demonstrating relaxation behavior over time. The relaxation came to equilibrium at higher frequencies, but not at the lowest frequencies. A viscoelastic response was also observed with hydrogels of the lowest gel fraction that correspondingly contained more water content.

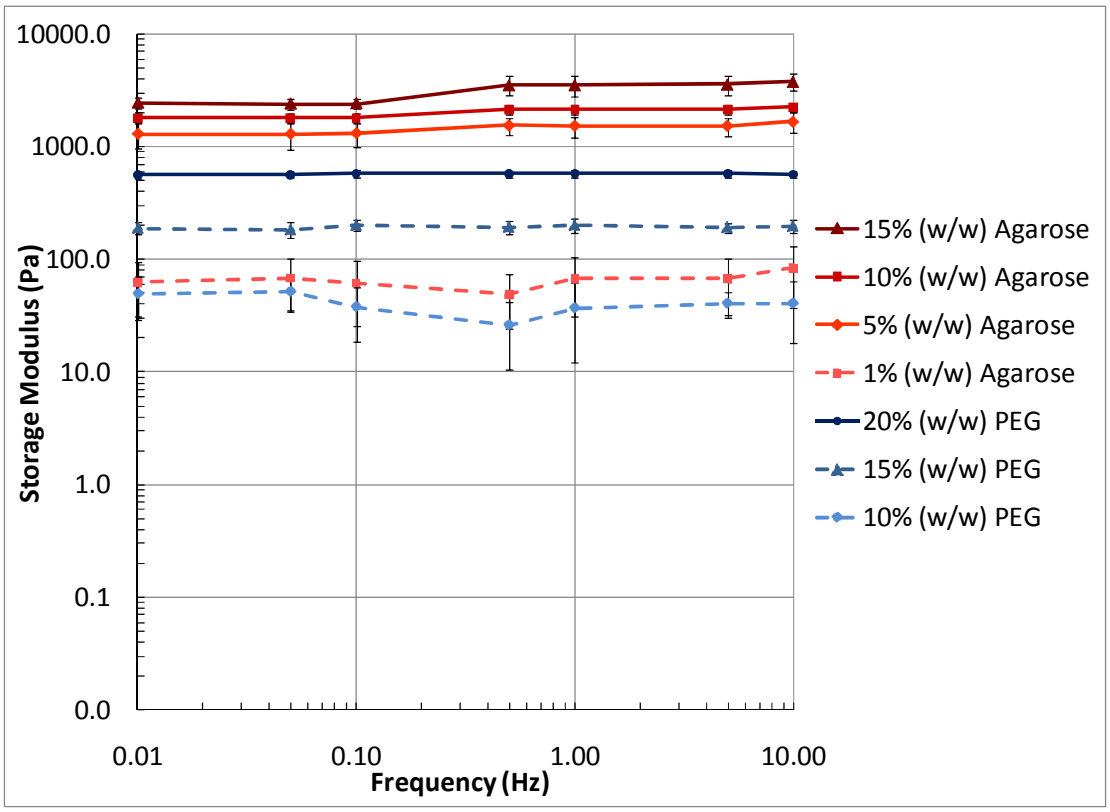

Figure 4.1: Storage modulus of agarose and PEG

The storage modulus gives an indication of material elasticity. All hydrogels in this study had storage moduli values that far exceeded their loss moduli values (*i.e.,* the hydrogels exhibited a dampening effect). Figure 4.1 illustrates that the 15, 10, and 5 weight percent agarose gels all possessed higher storage modulus values than any PEG gel. The 1% agarose and 10% PEG gels have a similar storage modulus. For agarose, the maximum and minimum storage modulus was approximately 3,500Pa (15% agarose) and 50Pa (1% agarose) respectively. Similarly for PEG hydrogels, the max and minimum storage modulus was roughly 570Pa (15% PEG) and 26Pa (10% PEG).

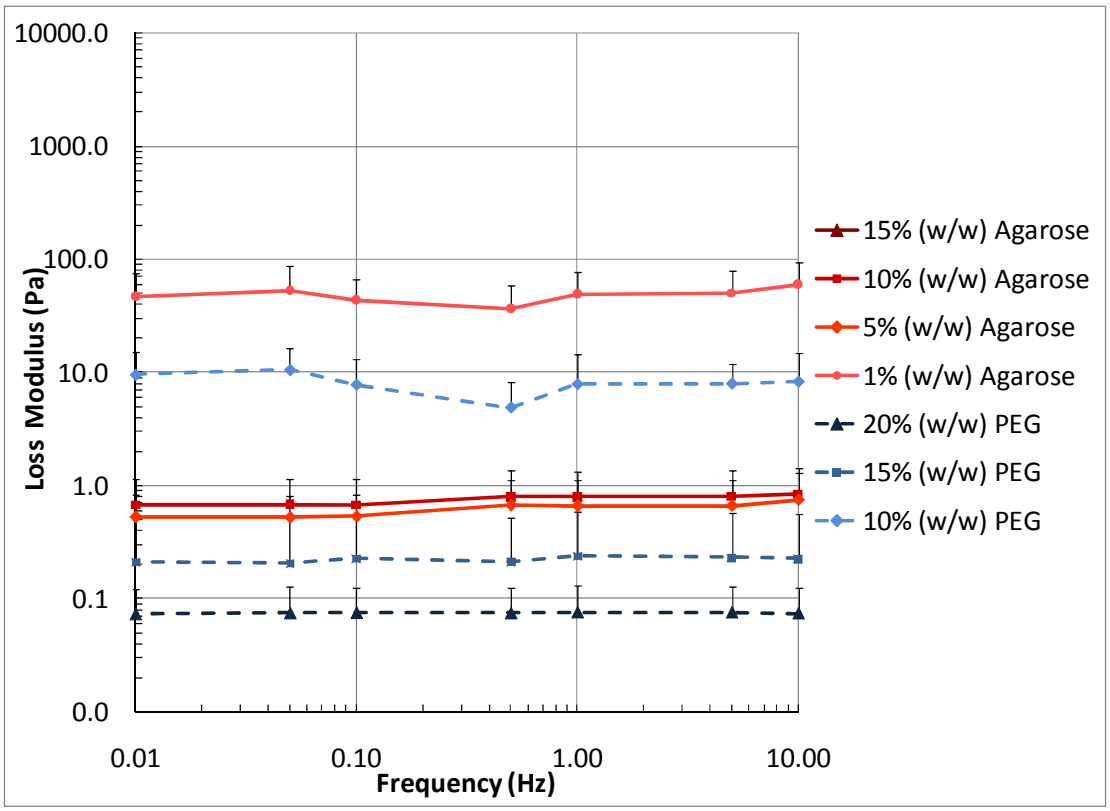

Figure 4.2: Loss modulus of agarose and PEG.

Figure 4.2 illustrates the loss modulus, or how much energy is absorbed by the sample over a given frequency range. The maximum and minimum values for agarose were 37Pa (1% agarose) and 0Pa respectively (Note – the 15% agarose cannot be included on a logarithmic plot with a value of zero). For PEG the maximum and minimum ranges were 11Pa (10% PEG) and 0Pa for (15% PEG).

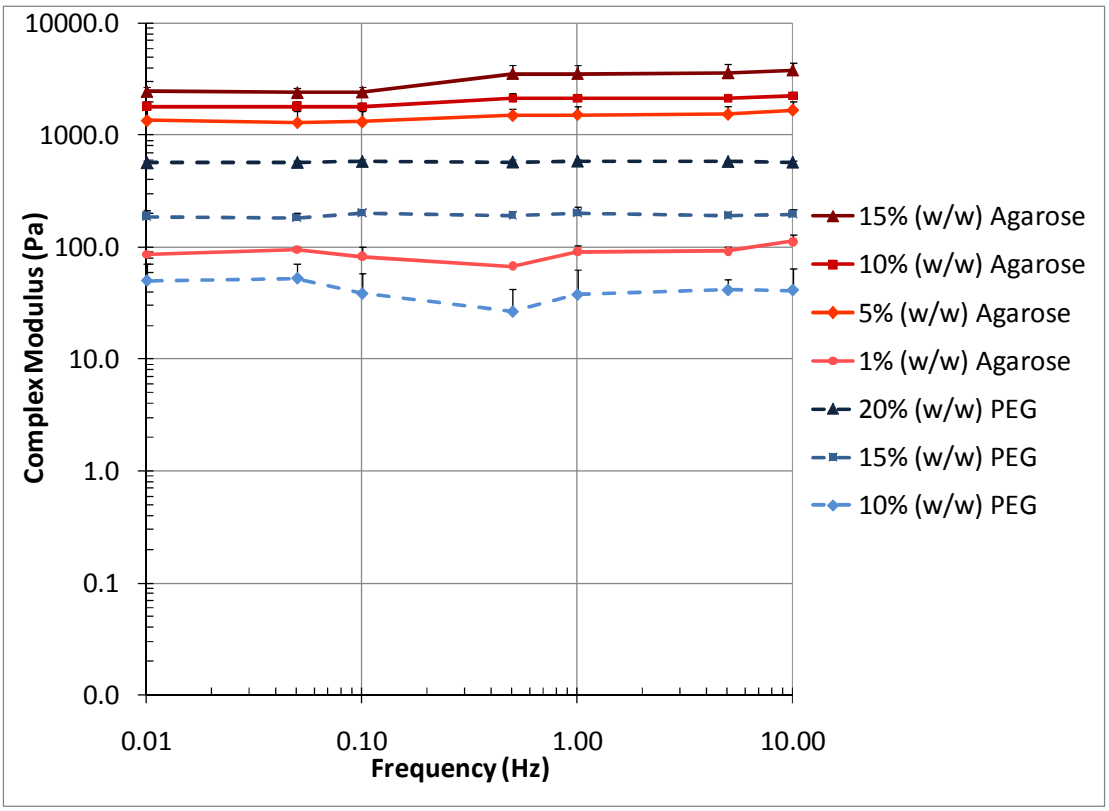

Figure 4.3: Complex modulus for agarose and PEG.

The complex modulus illustrates that higher weight percent gels positively correlate with higher complex modulus values. The agarose and PEG gels do not seem to respond too differently at increased frequencies. Recall from earlier that the complex modulus, G* is the magnitude of the storage (G_1) and loss (G_2) modulus. The maximum and minimum values of agarose were 3500Pa (15% agarose) and 67Pa (1% agarose) respectively. Similarly, the max and min values for PEG were 560Pa (20% PEG) and 26Pa (10% PEG) respectively.

4.3 Agarose, PEG and Wharton's Jelly Results

4.3.1 Equilibrium Modulus

Only one sample of Wharton's jelly produced incremental stress-relaxation data from which equilibrium modulus could be obtained at a value of ~-468Pa. The other

sample data was too noisy to decipher the results. The analysis of data from the Wharton's jelly is limited in this thesis. However, these limited data suggest that testing of additional, carefully harvested Wharton's jelly may produce samples that would be in the general range of moduli of the lowest weight percent agarose.

4.3.1.1 Statistics

Statistics were undeterminable for Wharton's jelly compared to the hydrogels due to poor resolution in data collection results.

4.3.2 Dynamic Modulus

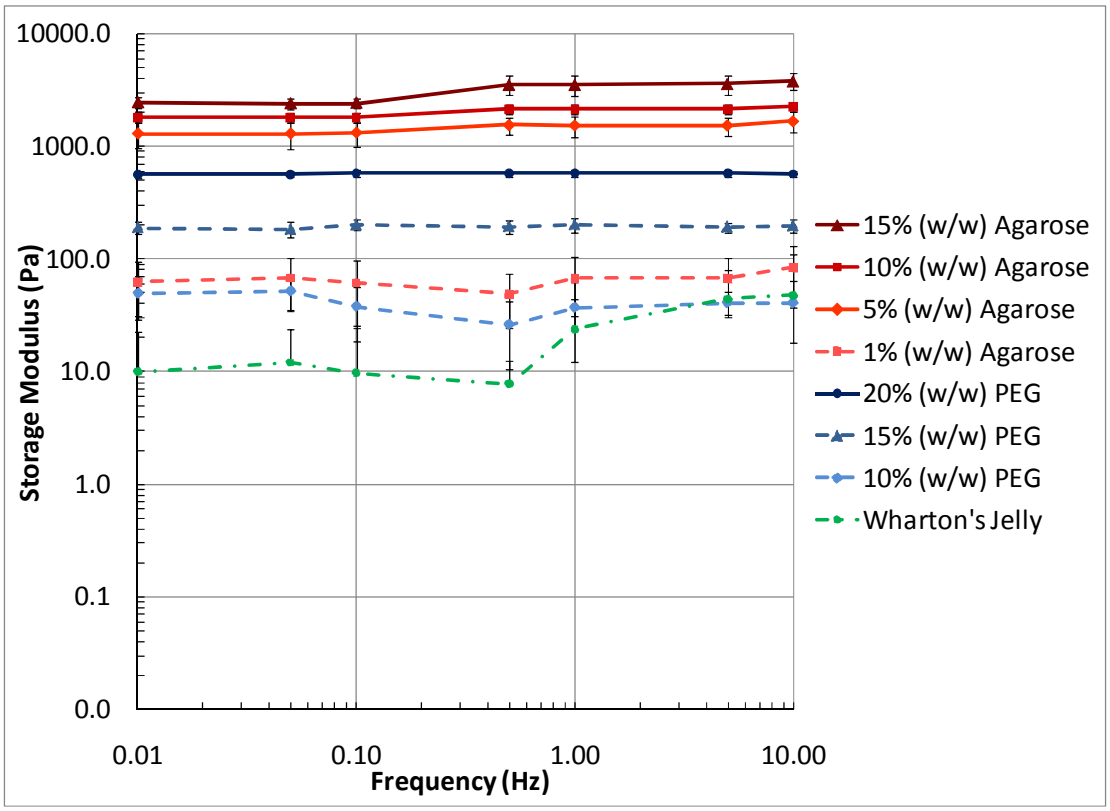

Figure 4.4: Storage modulus of agarose, PEG and Wharton's jelly.

Figure 4.4 shows the same trends that were seen in Figure 4.1, except the comparisons are made with the native tissue Wharton's jelly. It can be seen in Figure 4.4 that the Wharton's jelly had the least amount of stiffness at lower frequencies, but

interestingly increased in stiffness at higher frequencies. Caution should be noted that there were high standard deviations in the Wharton's jelly data where n=3 included highly variable data versus an n=3 with highly controlled gel samples.

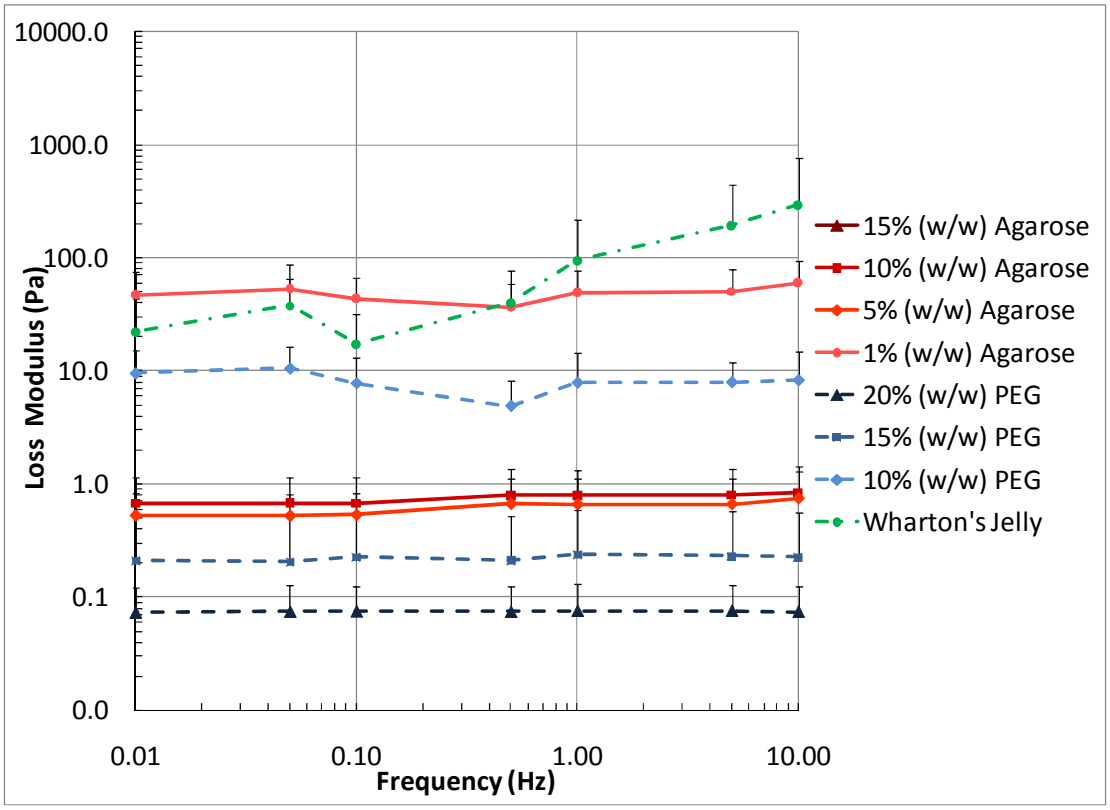

Figure 4.5: Loss modulus of agarose, PEG and Wharton's jelly.

The Wharton's jelly in Figure 4.5 also seems to show an increase in loss modulus with increasing frequencies. The 1% agarose most closely coincides with these loss modulus values and behavior.

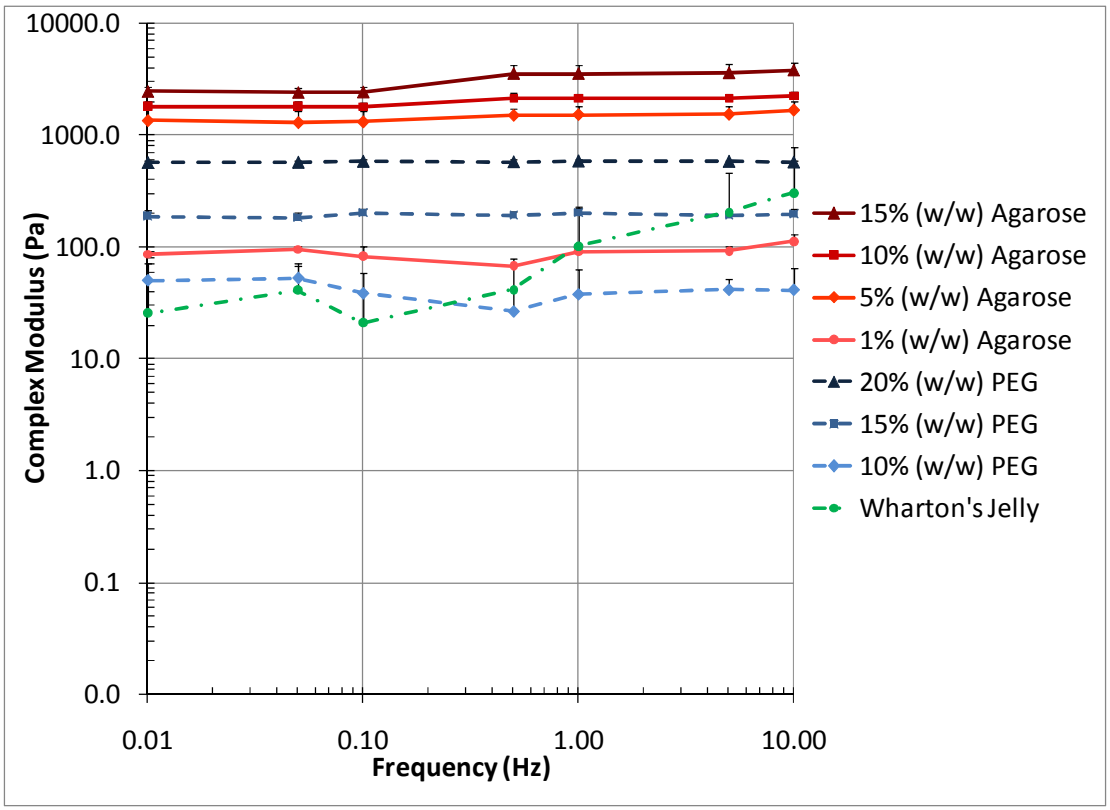

Figure 4.6: Complex modulus of agarose, PEG and Wharton's jelly.

Figure 4.6 shows the complex modulus with the incorporation of Wharton's jelly. Wharton's jelly also shows a viscoelastic response with modulus increasing with increased frequency. The 1% agarose shows a slight increase and the 10% PEG shows a slight decrease with increasing frequency.

4.4 Stress-Relaxation Behavior

Stress-relaxation was observed on all dynamics tests. Each specimen required extra time throughout the test cycle at each applied frequency to obtain equilibrium. Tests at lower frequencies seemed to reach equilibrium compared with higher frequencies that only approached equilibrium (refer to Appendix E).

5 Discussion

5. 1 Previous Work

It is known that tissue composition, ultrastructure and pathology have strong influences on tissue properties (Mow et al., 2004). Despite challenges to collect reliable data, it was theorized that proteoglycans, glycosaminoglycans, and hyaluronic acid would have a significant impact on tissue hydration and mechanical behavior comparing samples submerged in 70% EtOH versus PBS. Through experimentation, it was roughly shown that 70% EtOH submerged samples, of equine Wharton's jelly, had a stiffer toe region that climbed at a quicker rate up to 2500mN. Mechanically testing the removal of each protein or component would determine whether a correlation existed between a mechanical property such as modulus compared with percentage of water content, protein content/wet weight, or fixed charges within the tissue. From this information, conclusions about the roles water and fixed charges played within the tissue could be inferred (*i.e.,* the negatively charged molecules create a concentration gradient increasing the water content, which positively correlates with equilibrium modulus). Proteoglycans and GAGs re negatively charged due to sulfate and carboxyl groups and would be expected to attract water and alter the mechanical properties based on the fluid concentration inside a cell membrane. Water content can have a significant effect on the mechanical properties of soft tissues (Pennati, 2001), therefore further study investigating the roles each protein and component play in fluid retention is key to understanding viscoelastic responses and better ways to protect umbilical vessels.

During a creep test, viscoelastic behavior was noticed that may indicate interstitial fluid flow. As stress is applied to the tissue, the fluid is exuded out of the solid-porous matrix, presumably changing the charge density, and thus the mechanical behavior of the

tissue. Deformations in Wharton's jelly posses elasticity characteristics related to the glycoprotein microfibril network (Pennati, 2001). In articular cartilage, proteoglycans were found to be responsible for providing compressive stiffness (Mow et al., 2004). Once the phenomenon driving the mechanical response is solved, perhaps solutions to increasing the amount of Wharton's jelly in a developing womb may soon be found. Research combining tissue engineering of seeded hydrogels along with knowledge of growth factors present within Wharton's jelly could be combined to increase the amount of Wharton's jelly through fluidic injection.

5.2 Agarose vs. PEG

5.2.1 Static Testing Conclusions

The positive correlation between compressive stiffness and high weight percent hydrogels may be due to the hydrogels having smaller intermolecular spaces between the frequent chemical bonds, increasing the internal pressure within the gel making it increasingly harder to compress. The higher weight percent implies that more molecules must be packed into the same volume, thus making the solid matrix more dense and compact. The data presented in the equilibrium modulus results generally matches those found in the literature, demonstrating that agarose behaved predictably in our lab. Therefore, agarose serves as a suitable reference material for subsequent studies of other hydrogels and biological tissues of similar mechanical properties.

A comparison of agarose and PEG hydrogels enables the study of mechanical and chemical cross-linking, respectively. The values for equilibrium modulus in agarose far exceed those of similar weight percents of PEG hydrogels. There may be a higher number of physical crosslinks per chain in agarose compared with PEG. Despite the fundamental

differences between agarose and PEG, an increase in weight percent correlated with an increased modulus in both materials (Earnshaw et al., 2009).

It is difficult to directly compare equilibrium modulus values for like weight percent formulations of agarose and PEG due to the inherent differences in the molecular weights of molecules and the overall final structure of the hydrogel (Normand et al, 2000). It has been noted that equilibrium modulus values for agarose gels with the same weight percents can vary significantly depending on the source of agarose and batch-to-batch variations, type of agarose, testing method, and theoretical models used to obtain the modulus (Gu et al., 2003). However, the equilibrium modulus data described here for the higher weight percent PEG hydrogels further supports their use in tissue engineering applications for replacement cartilage (Earnshaw et al., 2009).

5.2.2 Dynamic Testing Conclusions

Complex modulus and phase angle shift from the frequency range (0.01 to 10Hz) was shown with increasing weight percents and loading frequency. These results corresponded with findings in the literature showing that as both frequency and hydrogel weight percent increased the complex modulus also increased (Gu et al., 2003; Chen et al., 2003). Literature also suggests a decrease in phase angle shift from gels with decreasing weight percent and loading frequency that was not observed in these thesis results (Gu et al., 2003). Large discrepancies were seen between the storage modulus and loss modulus, along with literature findings, proving that PEG and agarose hydrogels are largely elastic materials (Chen et al., 2003). The observed relaxation that did not come to equilibrium with the higher frequency applications may have relate to the time-dependent behavior of the hydrogels not having enough time to respond, this was most clearly seen at 10Hz.

Trends recognized in literature claim that increased dynamic stiffness with loading frequency for agarose hydrogels is similar to articular cartilage by the fluid pressurization effect (Gu et al., 2003). The fluid pressurization effect demonstrates that increased dynamic stiffness occurs when loading frequency (0.01-1Hz) is less pronounced for higher weight percents of hydrogels. Therefore, the fluid pressurization effect would decrease with higher gel weight percent and loading frequencies (Gu et al., 2003). Complex modulus results were in accordance, generally showing a slight increase in stiffness between 0.01-1Hz. The lowest weight percent hydrogels showed decreases in stiffness through this same range, which may be explained by too low of force-resolution from the instrumentation. The fluid pressurization effect was not observed in these thesis results at frequencies greater than 1Hz indicating a viscoelastic response from the hydrogels. It is hypothesized that as the water volume fraction of each hydrogel weight percent is an important consideration that needs to be pursued further. The relationship between water volume fraction and permeability would provide understanding of the biological responses of cells to interstitial fluid flow in hydrogel or cartilage under dynamic mechanical loading (Gu et al., 2003).

5.3 Hydrogels vs. Wharton's Jelly

Implications of this work may lead to pursuing the feasibility of synergistically using an injectable hydrogel and growth factors to increase the compressive stiffness of the umbilical cord in high risk pregnancies (*e.g.,* pre-eclampsia or lean cords**)**. However, Wharton's jelly currently proved to be a difficult material to test due to non-uniform geometry, internal coiling stresses, and the little amount of viable tissue that could be excised adjacent to vasculature. Preliminary results achieved in this thesis did not adequately provide comparisons between native tissue and hydrogels. This thesis work laid the foundation for developing a better comparison in the future. Results demonstrated that

Wharton's jelly possessed an unusually low compressive modulus compared to the lowest hydrogel weight percents used in this thesis (1% agarose and 10% PEG). However, the complex modulus of Wharton's jelly also appeared to positively correlate with higher frequencies, which suggest a viscoelastic response of the native tissue.

There are a variety of experimental techniques that have been used to characterize viscoelastic behavior in solid polymers with corresponding frequency ranges. The materials in this thesis were tested between 0.01 – 10Hz which is in the free oscillation pendulum technique range. Beyond this, the forced vibrations range (10^{-2} – 10^{3}Hz) is more complicated, but has a higher reproducibility in terms of extending testing predictions over a decade. If the hydrogels were tested at a very fast oscillation it is predicted to behave as a polymer in the forced vibrations, resonance range (10^{3} – 10^{4}Hz), or wave propagation regime (starting at 10^{4}Hz and beyond). On the other side of the spectrum, intersecting the free oscillation pendulum techniques range, stress relaxation and creep testing is generally performed (1 to > 10^{-6}Hz). In this study that frequency sweep data never seemed to reach equilibrium at smaller frequency ranges. This phenomenon with the specimens may have occurred due to the frequency range of testing (stress relaxation range) or may be due to time-dependent behavior of the hydrogel, which may not have had enough time to recover at quicker oscillations. Future studies should be done to confirm the hydrogels dynamic time dependent behavior over longer periods of time at higher frequencies. As either extreme of testing is encountered, testing becomes increasingly more sensitive to inaccuracies and variability (especially greater than 10kHz) (Ward & Sweeney, 2004). The range at which the hydrogels were tested in this thesis was carefully chosen to include simpler methods and practical applications of mechanical characterization for tissue engineering.

5.4 Overall Conclusions

This thesis research demonstrated the first documented comparison of agarose and PEG hydrogels being explored as cell carriers for tissue engineering applications. Although, PEG hydrogels and agarose are very different in terms of chemical structure, bond formation (chemical vs. physical), origin (synthetic vs. natural), and molecular weight, both hydrogels showed an increase in equilibrium modulus values with higher weight percent concentrations of hydrogels. Material type was not found to be significantly different, inferring that despite the differences between PEG hydrogels and agarose, both hydrogels performed similarly in terms of mechanical response, with the only significant difference being weight percent of each hydrogel. Although equilibrium moduli values for agarose hydrogels do not quantitatively match observations in the literature, a qualitative trend was found to be in accordance. The agarose hydrogels served as a guide to reference and attempt to validate the methods used to mechanically characterize both static and dynamic properties. These testing methods can be improved upon and perhaps used in the future to quantify mechanical properties of new materials and elucidate on how chemical cross-linking affects mechanical properties for hydrogels of interest.

PEG hydrogel has been proven to possess generally elastic properties similar to agarose, demonstrated by having high storage moduli (G_1) throughout the frequency range and strains employed in this study. In order for a material to be completely elastic, the material must always return to its original shape once the applied stress has been removed. All of the energy stored in the material as a result of the deformation would be entirely recoverable and the material would be independent to the rate of applied stress or strain (Mow et al., 2004). The results of the frequency sweep findings showed in all cases energy loss, where the amount of loss varied depending on the applied frequency. For both the

PEG and agarose, data showed the most energy dissipation at 5Hz. This means that if either material were implanted into a human joint, that material would dissipate the most amount of energy when a rate of movement of 5Hz were reached. At 10Hz, the applied impact would be too great to allow the material to respond appropriately in terms of dampening the shock on joints or Wharton's jelly resisting cord compression. Energy dissipation was found to dramatically decrease below 5Hz, positively correlating between frequency and energy loss.

5.5 Future Work

Future work will entail progressions from this thesis work with more controls and accurate methods for structured testing. More dynamic testing shall confirm stress relaxation phenomena at different frequencies and whether hydrogels possessing lower weight percentages reach equilibrium. If a stress relaxation trend is confirmed, the material properties can be checked by formulating an empirical equation based observed mechanical behavior and checked against constitutive equations. Once predicted and observed numerical relationships have been developed, these equations can be tested for validity by performing a creep test and seeing if the equations accurately predict creep behavior. Additionally, increasing the variety of test materials could lead to the discovery of a hydorgel with a balance of viscous and elastic properties that more closely characterize native tissue (*e.g.,* an agarose/PEG composite). More material property knowledge could allow future development of new materials and applications such as injection encapsulated osteoblasts for bone treatment.

Porous platens should enable easier fluid exudation and more compression of the solid matrix of the specimen. If a significant difference in mechanical properties existed

between a porous and non-porous platen, then this would help distinguish between pore size, charge densities or permeability playing a role in fluid retention.

The equilibrium swelling ratio provides information on the cross-linking density and polymer-solvent interaction parameter (amount of water content) (Bryant & Anseth, 2005). Unpublished work by Justine Roberts, in Dr. Stephanie Bryant's laboratory, shows differences in swelling ratios for both agarose and PEG hydrogels that agree with what is expected. A more tightly cross-linked material should have greater cross-linking retractile forces that result in less water absorption. As the cross-linking density (mol/l) increases, the compressive modulus increases and the volumetric swelling ratio decreases (Bryant & Anseth, 2005).

Comparisons between the swelling ratio's of Wharton's jelly to both types of hydrogels examined herein may provide interesting insight into the roles proteoglycans, hyaluronic acid, gylcosaminoglycans, pore size, and fixed charge density play in stimulating native tissues and hydrogels. Literature has found G_1 and G_2 to be slightly frequency dependent, verifying hydrogel usage in dynamic pressure stimulation for tissue engineering applications (Chen et al., 2003). Mechanical stimulation of tissue or hydrogels may aid in future drug delivery methods, which may include degradable polymers. Degradable polymers are important because they have many applications for tissue reconstruction and controlled drug delivery.

There are many potential applications for developing materials to match native tissues of choice as long as there is a method to provide feedback for testing these properties. Agarose hydrogels served an important first step in getting closer to determining the mechanical properties of Wharton's jelly. Research within has enabled a feedback mechanism for Professor Bryant's group, allowing for altering chemical

composition and observing the mechanical response through static and dynamic testing. This will enable the research group to tailor the chemical composition to obtain the desired mechanical response for the tissue engineering application of interest.

Bibliography

Bryant SJ and Anseth KS. Photopolymerization of Hydrogel Scaffolds: Scaffolding in Tissue Engineering: Chapter 6. CRC Press LLC, 2005.

Buttafoco L, Engbers-Buijtenhuijs P, Poot AA, Dijkstra PJ, Daamen WF, Van-Kuppevelt TH, Vermes I, and Feijen J. "First steps towards tissue engineering of small-diameter blood vessels: Preparation of flat scaffolds of collagen and elastin by means of freeze drying." Journal of Biomedical Material Research Part B Applied Biomaterials, 77(2):357-368, 2006.

Chen Q, Suki B, and An KN. "Dynamic mechanical properties of agarose gels modeled by a fractional derivative model." Journal of Biomechanical Engineering, 126(5):666-671, 2004.

Earnshaw A, Roberts JJ, Nicodemus GD, Bryant SJ, and Ferguson VL. "The Mechanical Behavior of engineered Hydrogels." ASME 2009 Summer Bioengineering Conference. Ahead of publication.

Gervaso F, Pennati G, Boschetti F, Rigano S, Pigni A, and Padoan A. "Biomechanics of the human umbilical cord under compressive loads." 2003 Summer Bioengineering Conference, 931-932.

Gu WY, Yao H, Huang CY, and Cheung HS. "New insight into deformation-dependent hydraulic permeability of gels and cartilage and dynamic behavior of agarose gels in confined compression." Journal of Biomechanics, 36:593-598, 2003.

Herberhold C, Faber S, Stammberger T, Steinlechner M, Putz R, Englmeier KH, Reiser M, and Eckstein F. "In situ measurement of articular cartilage deformation in intact femoropatellar joints under static loading." Journal of Biomechanics, 32(12):1287-1295, 1999.

Humphery JD and Delang SL. An introduction to biomechanics solids and fluids, analysis and design. New York: Springer Science and Business Media LLC, 2004.

Kaab MJ, Ito K, Clark JM, and Notzli HP. "Deformation of articular cartilage collagen structure under static and cyclic loading." Journal of Orthopedics Research,16(6):743-751,1998.

Lakes RS. Viscoelastic Solids. CRC Press LLC, 1998.

Lin-Gibson S, Bencherif S, Cooper JA, Wetzel SJ, Antonucci JM, Vogel BM, Horkey F, and Washburn NR. "Synthesis and characterization of PEG Dimethacrylates and their Hydrogels." Biomacromolecules, 5(4):1280-1287, 2004.

Marcu L, Cohen D, Maarek JI and Grundsfest WS. "Characterization of type I, II, III, IV, and V collagens by time-resolved laser-induced fluorescence spectroscopy." SPIE--the International Society for Optical Engineering, 3917:93-101, 2000.

Mase GE. Schaum's Outline: Continuum Mechanics. McGraw-Hill, 1970.

Matthews LS, Sonstegard DA, and Henke JA. "Load bearing characteristics of the patella-femoral joint." Acta Orthopaedica Scandinavica, 48(5):511-516, 1977.

Mauck RL, Seyhan SL, Ateshian GA, et al. "Influence of seeding density and dynamic deformation loading on the developing structur/function relationships of chondrocyte-seeded agarose hydrogels." Annals of Biomedical Engineering, 30(8):1046-1056, 2002.

Mow VC, Gu WY, and Chen FH. "Structure and function of Articular Cartilage and Meniscus." In: Mow VC, and Huiskers. Basic orthopaedic biomechanics & mechano-biology. Lippincott Williams & Wilkins 3rd Edition, 2004.

Mow VC, Kuei SC, Lai WM, and Armstorng CG. "Biphasic creep and stress relaxation of articular cartilage in compression? Theory and experiments." Journal of Biomechanical Engineering, 102(1):73-84, 1980.

Myers JC, Li D, Amenta PS, Clark CC, Nagaswami C, and Weisel JW. "Type XIX collagen purified from human umbilical cord is characterized by mulitple sharp kinks delineating collagenous subdomains and by intermolecular aggregates via globular, disulfide-linked, and heparin-binding amino termini." The Journal of Biological Chemistry , 278(3):32047-3205, 2003.

Nicodemus GD and Bryant SJ. "The role of hydrogel structure and dynamic loading on chondrocyte gene expression and matrix formation." Journal of Biomechanica, 41(7):1528-1536, 2008.

Normand V, Lootens DL, Amici E, Plucknett KP and Aymard P. "New insight into agarose gel mechanical properties." Biomacromolecules. 1(4):730-738, 2000.

Park S, Hung CT, and Ateshian GA. "Mechanical response of bovine articular cartilage under dynamic unconfined compression loading at physiological stress levels." Osteoarthritis and Cartilage. 12(1):65-73, 2004.

Pennati G. "Biomechanical properties of the human umbilical cord." Biorheology. 38:355-366, 2001.

Rowley JA, Madlambayan G, and Mooney DJ. "Alginate hydrogels as synthetic extracellular matrix materials." Biomaterials, 20(1):45-53, 1999.

Saris DB, Mukherjee N, Berglund LJ, Schultz FM, An KN, and O'Driscoll SW. "Dynamic pressure transmission through agarose gels." Tissue Engineering, 6(5):531-537, 2000.

Sawhney AS, Pathak CP, and Hubbell JS. "Bioerodible hydrogels based on photopolymerized poly(ethylene glycol)-co-poly(alpha-hydroxy acid)diacrylate macromers. " Macromolecules, 26(4):581-587, 1993.

Scandiucci de Freitas P, Wirz D, Stolz M, Gopfert B, Friederich N-F and Daniels AU. "Pulsatile dynamic stiffness of cartilage-like materials and use of agarose gels to validate mechanical methods and models." Journal of Biomedical Materials Research Part B: Applied Biomaterials, 78(B):347-357, 2006.

Skulstad SM. Thesis:Umbilical vein constriction at the abdominal wall: An ultrasound study in low risk pregnancies. Norway:Universitas Bergensis, 2005.

Ward IM and Sweeney J. An Introduction to the Mechanical Properties of Solid Polymers (2nd Edition): CH 5 the Measurement of Viscoelastic Behavior. John Wiley and Sons, Ltd, 2004.

Villanueva I, Klement BJ, Von Deutsch D, and Bryant SJ. "Cross-linking density alters early metabolic activities in chondrocytes encapsulated in poly(ethylene glycol) hydrogels and cultured in the rotating wall vessel." Biotechnology Bioengineering, 102(4):1242-1250, 2008.

Vizza E, Correr S, Goranova V, Heyn R, Angelucci PA, Forleo R, and Motta PM. "The collagen skeleton of the human umbilical cord at term. A scanning electron microscopy study after 2N-NaOH maceration." Reproduction, Fertility and Development, 8(5): 885-894, 1996.

Appendix A

PEGDM

Calculations for PEGDM (0.3g/ml PBS):

PI (0.6 wt% stock), 10 wt% gel, assume 1 g at a density of 1g/ml.

Convert grams to fluid equivalent:

0.1 g PEGDM = 100µl PEGDM & 0.9g PBS = 900µl PBS which gives 1000µl.

Calculation for a 10wt% gel:

Use 0.05 wt% PI

grams PI 0.05/100 (1g) = 0.0005 g PI

(0.005g PI)/(0.006g/ml PBS)*(1000µl/1ml) =83.3µl PI

(900-83.3)µl = 817µl PBS

(0.1g)(0.3g/ml PBS) = 817µl PBS

(0.1g)(0.3g/ml PBS) =0.33ml = 333µl PEGDM

(817-333)µl = 483µl PBS

5*5=25 gels * 85µl

10 gels = 850µl

(850µl)/900*(83.3µl) = 80µl (proportion calculation)

For wt% PEGDM 0.3g/ml PBS use the density to figure out how much solution to add for wt % calculations.

Calculation for 15 wt% gel:

Use 0.022% PI

Calculation for 20 wt% gel:

Use 0.0125% PI

Appendix B

Potential Sources of Error with Test Methods

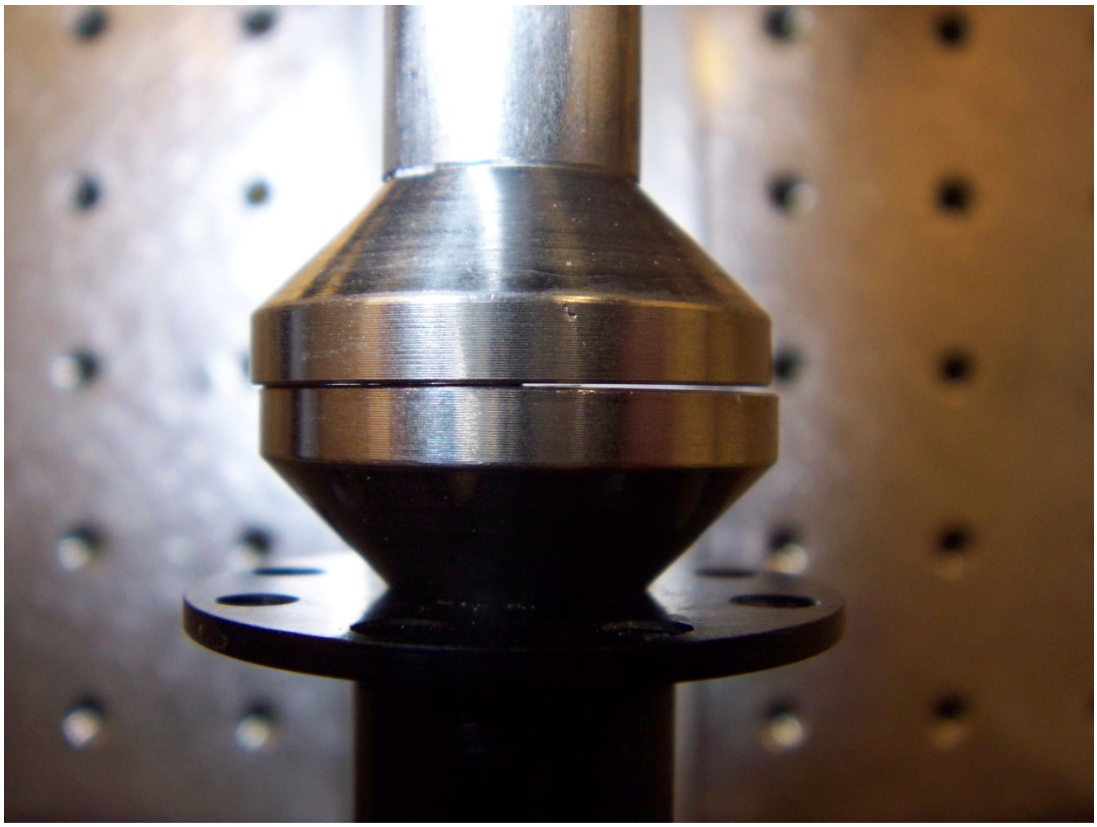

Figure B.1: Misalignment of test fixture caused error in testing.

Figure B.1, illustrates that the compression platens were off axis during testing. The most pronounced error occurred during dynamic testing over a two hour period. It is predicted that this made it harder to achieve equilibrium and could explain the stress relaxation behavior observed in the results.

Appendix C

Matlab Code for Equilibrium Modulus

```
clear all
 close all
cd('C:/Users/Audrey/Desktop/Bose Research/Data/agarose') %references where files are
located
data=dlmread('2008_11_12_agarose1_gel21_equilibmod__metal1.CSV'); %reads my files &
uploads into matlab
%dlread command to read a file
%Column titles: Points; Elapsed Time (Sec); Scan Time (Sec); Disp (mm);
%Load (g)
%rate to find data equilibrium is 1g/min
%all of the data for that slope 1 g/min (load vs. time)= 0.016667 g/s
%calculating the equilibrium modulus at each interval of strain
%5%,10%,15%,20%
dia=4.40e-3;  %m
label1=['EM, A1, Gel21, Stress (Pa) Vs. Time (s)'];
label2=['EM, A1, Gel21, Stress (Pa) Vs. Strain (%)'];
strain=[.05,.1,.15,.2];
smoothing =10;                          %change the amount of smoothing for the data
data(:,5)=abs(data(:,5));  %g           % original signal
x=data(:,5) ;                           % I have chosen h=3
y=smooth(x,smoothing);                  %calls smoothing function (must have this saved in
work space)
 % plot(y,'r');
% hold on
% plot(x,'g')
low_slope = 0;                          %start at zero
curr_data = [];                         %create empty matrix to store the current data
means = [];                             %create the matrix to store loads
mean_times = [];                        %creat matrix to store times
        for i = smoothing:size(y,1)-1   %ignoring the first and last data points
                slope = abs((y(i) - y(i-1)) / (data(i,3) - data(i-1,3)));
%calculates slope of load vs time
                if slope <= .016667
                        curr_data = [curr_data; data(i, 3:5)]; %record data
                        low_slope = 1;          %if at the low slope start recording the data
                end
                if slope > .016667 && low_slope == 1
%short circuit & if false it doesn't evaluate (else if)
                        m = mean(curr_data(:,3));
                        if isempty(find(abs(means-m)./means <= 0.01))
                                means = [means; mean(curr_data(:,3))];
%stores range of values in means(load) array, takes mean of data to get mean load
                                mean_times = [mean_times; mean(curr_data(:,1))];
```

```
%does the same thing for time
                        end
                        curr_data = [];
%only records data where the slope is low = 1
                        low_slope = 0;
%because not at low slope
                end
        end
        if low_slope == 1
                means = [means; mean(curr_data(:,3))];
%stores range of values in means(load) array, takes mean of data to get mean load
                mean_times = [mean_times; mean(curr_data(:,1))];
%does the same thing for time
        end
% means=means([1,2,5,8]);
%use these two lines to take out points that you don't want in the regression
% mean_times=mean_times([1,2,5,8]);
area=(dia/2)^2*pi;
stress=means*(1e-3)*9.8/area/(1e3);
%convert load to stress kg*m/s^2/m^2/E-3
subplot(2,2,1:2)
plot(data(:,3), data(:,5)*9.8/area/(1e6))
hold on
plot(data(:,3),y*9.8/area/(1e6),'--r')
hold on
scatter(mean_times, stress,'o');
xlabel('Time (s)')
ylabel('Stress (kpa)')
title(label1)
legend('Measured Stress','Least Squares Fit (Stress)','Mean Stress @ 1g/min')
%plot stress vs. strain
[a1,a0]=LinearRegression(strain',stress);
%calls regression function (must have this saved in the workspace
subplot(2,2,3:4)
plot(strain,stress,'o')
hold on
x1=[min(strain):.01:max(strain)];
plot(x1,a1.*x1+a0,'-r')
title(label2)
xlabel('% Strain')
ylabel('Stress (kPa)')
legend('Linear Modulus','Slope =  kPa')
display('slope')
a1
% saveppt('WJ_Gel9',label2)
```

Appendix D

Matlab Code for Frequency Sweep

```
clear all
close all
cd('C:/Users/Audrey/Desktop/Bose Research/Data/agarose') %refernces where files are
located
data=dlmread('2008_11_15_agarose10_gel39_freqsweep__metal1.CSV'); %reads my files &
uploads into matlab
%dlread command to read a file
diameter=3.1e-3;                    %m CHANGE THIS
height=3.1e-3;                      %m CHANGE THIS
% ip0=.753e-3;                     %initial m at 0g load
initial=[3.75, 6.5, 28, 50, 328, 675, 3500];
final=[4.1, 8.2, 33, 65, 385, 750, 3750];
start=-399;
freq=[10, 5, 1, .5, .1, .05, .01];
for duck=1:7
        clear current_data new10Hz ;
        start=start+400;
        current_data=(data(start:start+399,1:5));
        %collect terms at the maximum values between the set interval
        [m,n]=size(current_data);
%fits the new matrix to be created into the appropriate size
        %all of the data for that frequency
        i10Hz = current_data(find(and(current_data(:,1) >= 1, current_data(:,1) <=
start+399)),:);
         %makes a new matrix for the interested time interval
        new_data=current_data(find(and (current_data(:,3)>=initial(duck),
current_data(:,3)<=final(duck))),:);
        new10Hz = new_data(:, 3:5);
        t(duck)=final(duck)-initial(duck);  %time period over which the delta is calculated in
seconds
        figure(duck);
        subplot(2,2,1:2);
        [AX,H1,H2]=plotyy(i10Hz(:,3),i10Hz(:,5),i10Hz(:,3),i10Hz(:,4));
        set(0,'DefaultAxesYColor','k')
        set(get(AX(1),'Ylabel'),'String','Load (g)')
        set(get(AX(2),'Ylabel'),'String','Displacement (mm)')
%       set(gca,'ylim',[min(-100),max(-70)])
        xlabel('Time (s)')
        label1=['FS, 10% Agarose, 10% Strain,' num2str(freq(duck)) 'Hz Vs. Time (s)'];
%CHANGE THIS
        title(label1)
```

```
        [x,y]=size(new10Hz);            %fits the new matrix to the size of the matrix just
created; max(new10Hz(:,3);
        yload10=new10Hz(:,3);
        ydisp10=new10Hz(:,2);
        xtime10=new10Hz(:,1);

        label2=['FS, 10% Agarose, 10% Strain,' num2str(freq(duck)) 'Hz Vs. Time (s)']; %
%CHANGE THIS
        subplot(2,2,3:4);
        [AX,H1,H2]=plotyy(xtime10,yload10,xtime10,ydisp10);
        set(0,'DefaultAxesYColor','k')
        set(get(AX(1),'Ylabel'),'String','Load (g)')
        set(get(AX(2),'Ylabel'),'String','Displacement (mm)')
        xlabel('Time (s)')
        title(label2)
        %maximum values of load collect g
        loadmax=new10Hz(find(and(new10Hz((2:x-1),3)>new10Hz((1:x-2),3), new10Hz((2:x-
1),3)>=new10Hz((3:x),3)))+1,1:3);
        %minimum values of load collect g
        loadmin=new10Hz(find(and(new10Hz((2:x-1),3)<new10Hz((1:x-2),3), new10Hz((2:x-
1),3)<=new10Hz((3:x),3)))+1,1:3);
        %values of maximum displacement, collect mm
        dispmax=new10Hz(find(and(new10Hz((2:x-1),2)>new10Hz((1:x-2),2), new10Hz((2:x-
1),2)>=new10Hz((3:x),2)))+1,1:2);
        %values of minimum displacment, collect mm
        dispmin=new10Hz(find(and(new10Hz((2:x-1),2)<new10Hz((1:x-2),2), new10Hz((2:x-
1),2)<=new10Hz((3:x),2)))+1,1:2);
        %determines the size of the matrices based on where it starts in load
        %or displacement
%       if size(loadmax)>size(dispmax)   %adjust to size of matrix for
%       subtraction & calculates time
        for i=1:min([size(dispmax,1), size(loadmax,1)])
                time(i,:)=[loadmax(i,1)-dispmax(i,1)];
%time between two peaks (load and displacement), used later
        end
        delta=abs((2*pi()*time*freq(duck)))
        mean_delta(duck)=mean(delta)
        %finding the initial loads, g
        for i=1:min([size(loadmin,1), size(loadmax,1)])
                iload(i,:)=-abs([(loadmax(i,3)-loadmin(i,3))/2]); %amplitude of load
  end
   meaniload(duck)=mean(iload(duck))*10^-3; %mean value of load in kg
    %stress calculations, Pa
        area=(((diameter)/2)^2)*pi;     %cross-sectional area in m^2
        istress=(meaniload)/area*9.8;   %stress = force/area in Pa, Note raw data is
converted to meters here
        stress=istress(duck)*sin(2*pi*freq(duck).*new10Hz(:,1));
  %finding the initial displacements mm
```

```
        for i=1:min([size(dispmin,1), size(dispmax,1)])
                        idisp(i,:)=[(dispmax(i,2)-dispmin(i,2))/2]; %this is the average
displacement (from amplitude of displacement)
  end
  meanidisp(duck)=mean(idisp(duck))*10^-3; %mean displacement in meters

  %strain calculations
  istrain=(meanidisp./height);
        strain=istrain(duck)*sin(2*pi*freq(duck).*new10Hz(:,1)-mean_delta(duck));
        G1=(istress.*cos(mean_delta(duck)))./istrain./1e3;
        G2=(istress.*sin(mean_delta(duck)))./istrain./1e3;
        tanD=G1./G2;
        G_star=sqrt(G1.^2+G2.^2); %Awad HA, FUNCTIONAL PROPERTIES OF BIOMATERIALS
FOR %CARTILAGE TISSUE
% ENGINEERING USING ADIPOSE DERIVED ADULT STEM CELLS
%    G_star=G1+G2; %source introduction to mechanical properties of solid polymers
        hold off
        label3=['FS, 10% Agarose, 10% Strain,' num2str(freq(duck)) 'Hz, Stress (Pa) Vs. Strain
(%)'];
% CHANGE THIS
        figure(8);
        subplot(4,2,duck);
        plot(strain(:,:),stress(:,:)./1e3)
%       set(gca,'ylim',[min(10.5),max(13)])
%       set(gca,'xlim',[min(.905),max(.945)])
        xlabel('Strain (%)')
        ylabel('Stress (Pa)')
        title(label3)
end
for duck=1:7
        figure(9);
        subplot(2,2,1:2)
        label4=['FS, 10% Agarose, 10% Strain, G_1,G_2 Vs. Frequency (Hz)']; % CHANGE THIS
        [AX,H1,H2]=plotyy(freq,G1,freq,G2);
        set(0,'DefaultAxesYColor','k')
        set(get(AX(1),'Ylabel'),'String','G1 (kPa)')
        set(get(AX(2),'Ylabel'),'String','G2 (kPa)')
        xlabel('Frequency (Hz)')
        title(label4)
%       set(gca,'ylim',[min(10.5),max(13)])
%       set(gca,'xlim',[min(.905),max(.945)])
        subplot(2,2,3:4)
        label5=['FS, 10% Agarose, 10% Strain, tanD, G* Vs. Frequency (Hz)']; % CHANGE
%THIS
        [AX,H1,H2]=plotyy(freq,tanD,freq,G_star);
        set(0,'DefaultAxesYColor','k')
        set(get(AX(1),'Ylabel'),'String','tanD')
        set(get(AX(2),'Ylabel'),'String','G_star (kPa)')
```

```
        xlabel('Frequency (Hz)')
        title(label5)
end
display('G1')
abs(G1)
display('G2')
abs(G2)
abs(tanD)
G_star
```

Appendix E

Matlab Figures of Dynamic Modulus

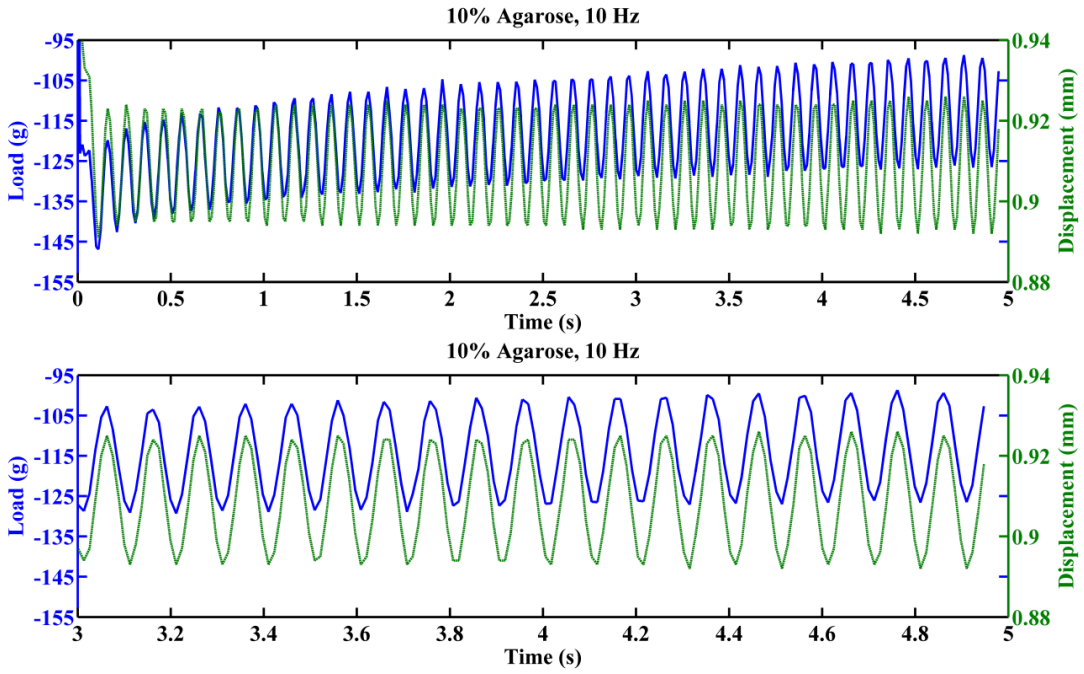

Figure E.1: The top image displays raw frequency sweep data above at 10Hz on 10% agarose hydrogel. The bottom figure displays the selected range of equilibrium that was used for calculation purposes.

The equilibrium slope near the end of 10Hz is higher than the equilibrium slope seen at 0.01Hz. It can be seen in the above figure that stress relaxation occurs as the force relaxes with a "semi-constant" or repetitive displacement over time.

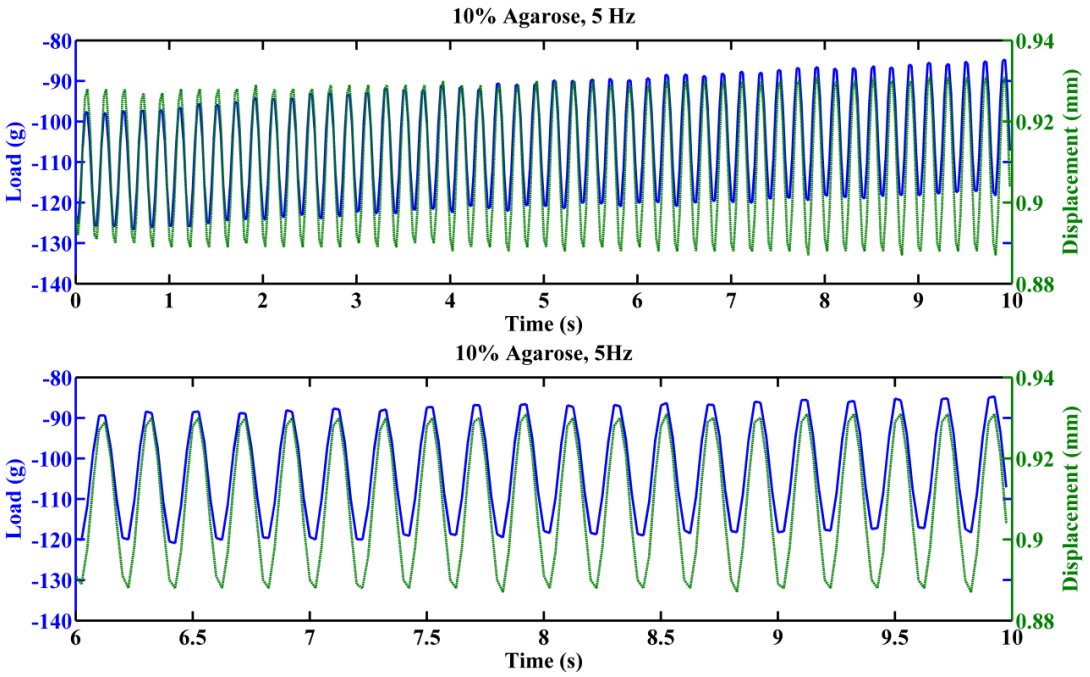

Figure E.2: The top image displays raw frequency sweep data above at 5Hz on 10% agarose hydrogel. The bottom figure displays the selected range of equilibrium that was used for calculation purposes.

It can be seen in the above figure that stress relaxation occurs as the force relaxes with a "semi-constant" or repetitive displacement over time.

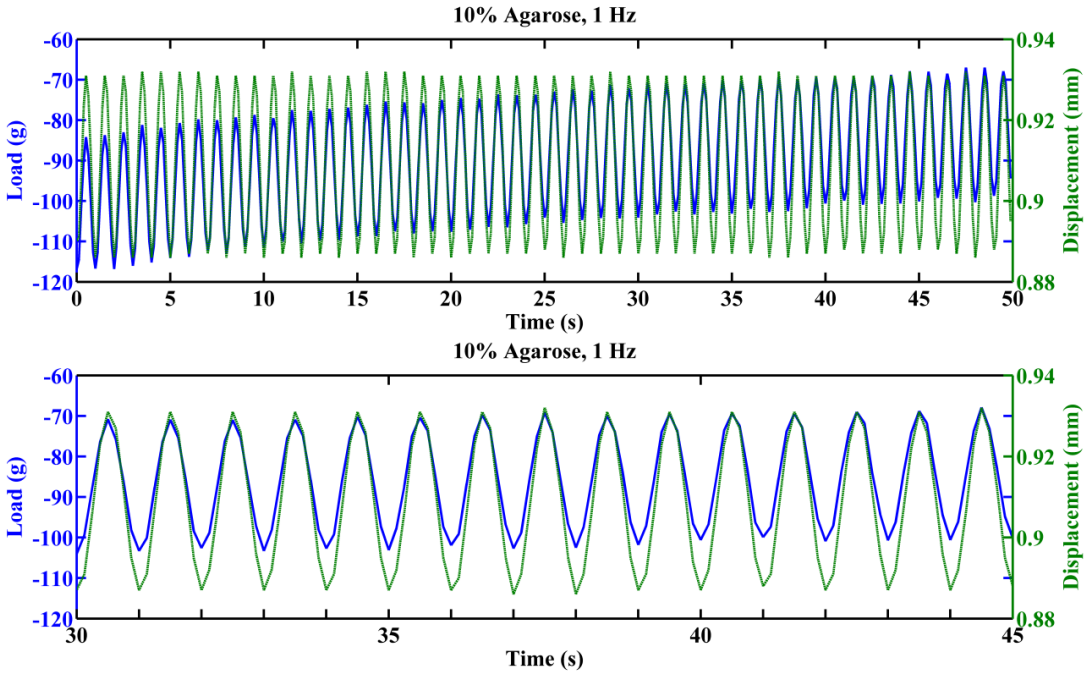

Figure E.3: The top image displays raw frequency sweep data above at 1Hz on 10% agarose hydrogel. The bottom figure displays the selected range of equilibrium that was used for calculation purposes.

It can be seen in the above figure that stress relaxation occurs as the force relaxes with a "semi-constant" or repetitive displacement over time.

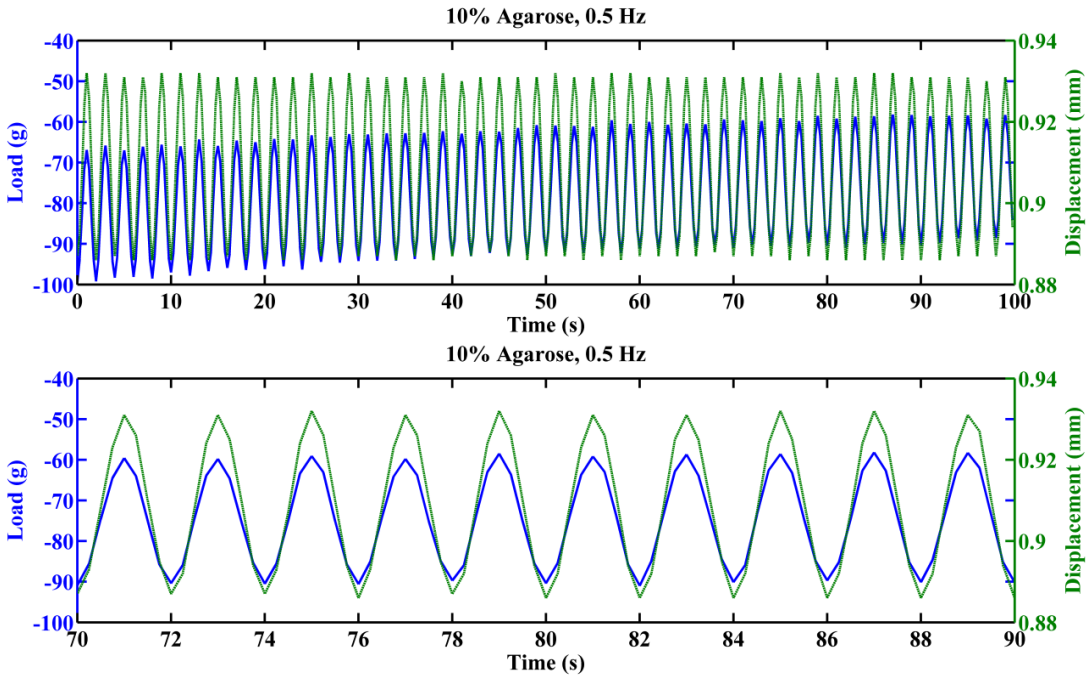

Figure E.4: The top image displays raw frequency sweep data above at 0.5Hz on 10% agarose hydrogel. The bottom figure displays the selected range of equilibrium that was used for calculation purposes.

It can be seen in the above figure that stress relaxation occurs as the force relaxes with a "semi-constant" or repetitive displacement over time.

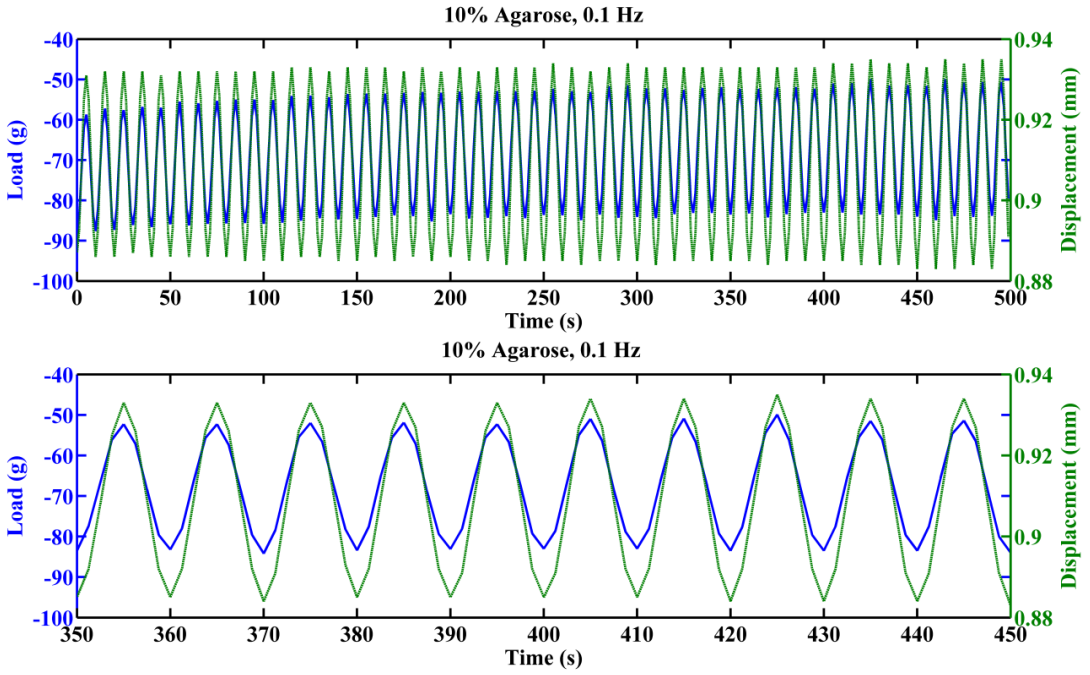

Figure E.5: The top image displays raw frequency sweep data above at 0.1Hz on 10% agarose hydrogel. The bottom figure displays the selected range of equilibrium that was used for calculation purposes.

It can be seen in the above figure that stress relaxation occurs as the force relaxes with a "semi-constant" or repetitive displacement over time.

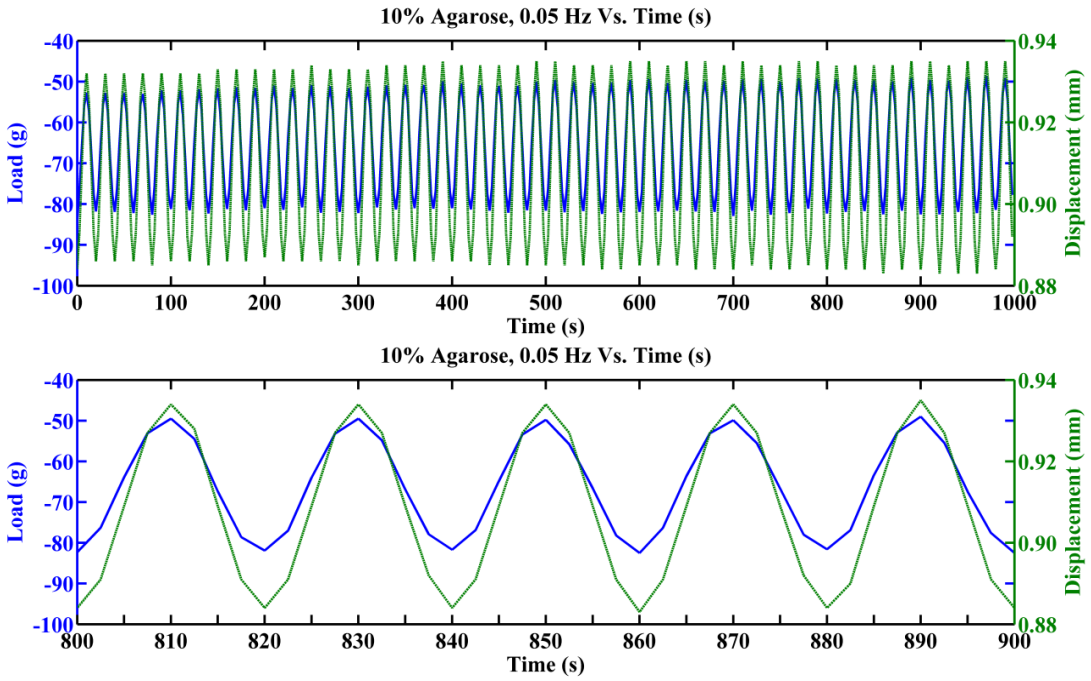

Figure E.6: The top image displays raw frequency sweep data above at 0.05Hz on 10% agarose hydrogel. The bottom figure displays the selected range of equilibrium that was used for calculation purposes.

It can be seen in the above figure that stress relaxation occurs as the force relaxes with a "semi-constant" or repetitive displacement over time.

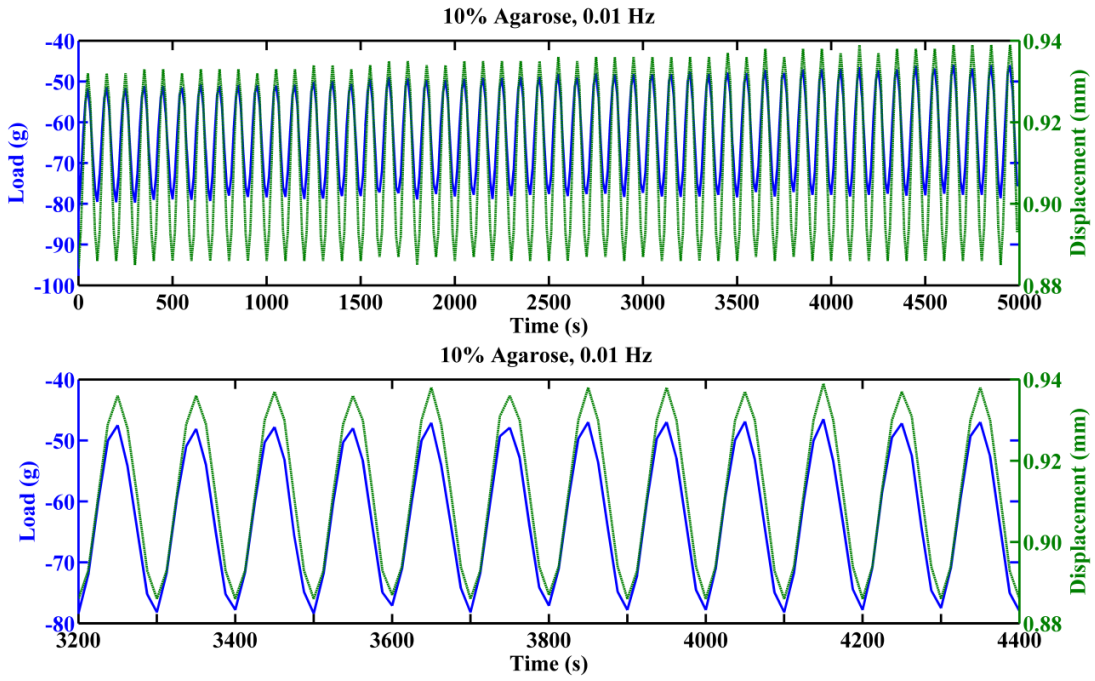

Figure E.7: The top image displays raw frequency sweep data above at 0.01Hz on 10% agarose hydrogel. The bottom figure displays the selected range of equilibrium that was used for calculation purposes.

It can be seen in the above figure that stress relaxation occurs as the force relaxes with a "semi-constant" or repetitive displacement over time.

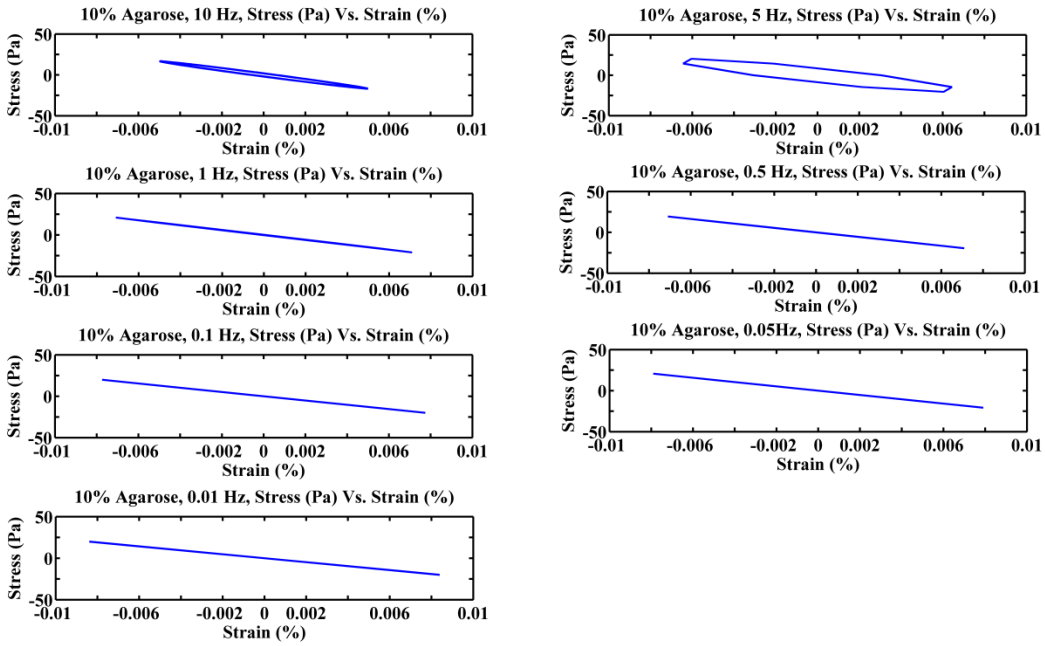

Figure E.8: This shows the amount of loss that occurred during testing at each frequency.

These figures show time dependent viscoelastic responses of the specimen tested. These figures indicate very little loss, but high energy dissipation at 5Hz and hardly any at 10Hz.

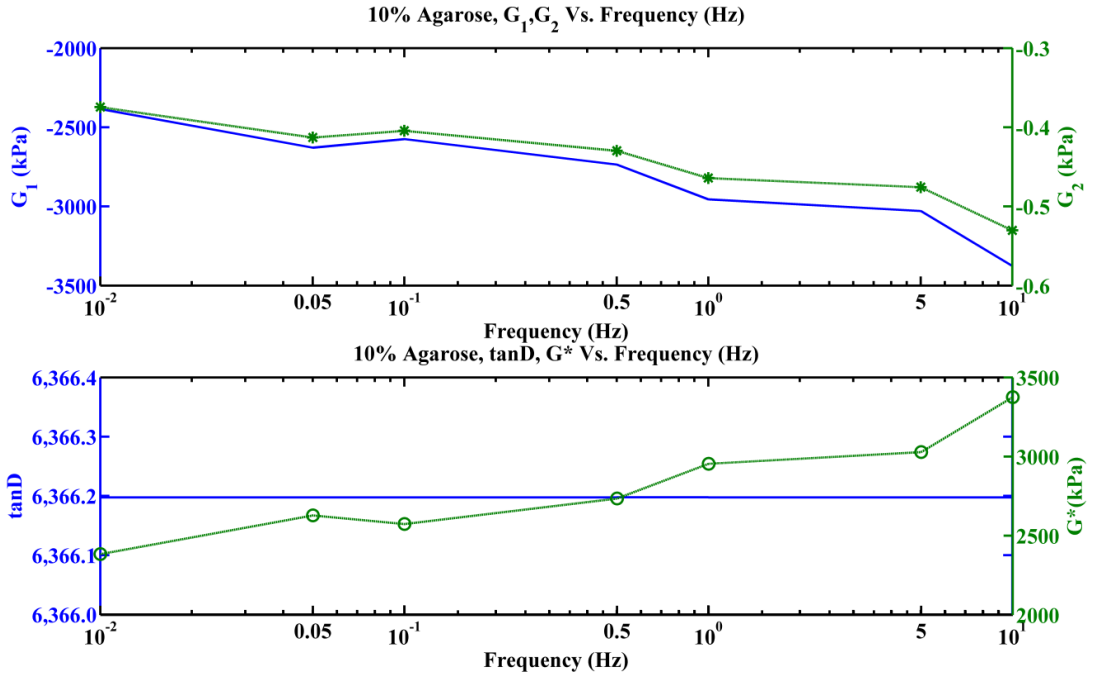

Figure E.9: This displays the overall storage (G_1, solid) and loss (G_2, star) moduli over the seven different logarithmically varying frequencies.

The figure on the bottom of E.9 displays tanD (G_1/G_2, solid) and the complex modulus (G*, circles) over the seven logarithmically varying frequencies. The complex modulus increases while the ratio between the storage and loss modulus remain the same.